

# 1 Post-stroke changes in brain structure and function can both 2 influence acute upper limb function and subsequent recovery

3

4 Catharina Zich<sup>1,2,3</sup>, Nick S Ward<sup>1</sup>, Nina Forss<sup>4,5</sup>, Sven Bestmann<sup>1,6</sup>, Andrew J Quinn<sup>7</sup>, Eeva  
5 Karhunen<sup>8</sup>, Kristina Laaksonen<sup>4,8</sup>

6

7 Affiliations:

8 <sup>1</sup>Department of Clinical and Movement Neuroscience, UCL Queen Square Institute of Neurology, United  
9 Kingdom

10 <sup>2</sup>Wellcome Centre for Integrative Neuroimaging, FMRIB, Nuffield Department of Clinical Neurosciences,  
11 University of Oxford, United Kingdom

12 <sup>3</sup>Medical Research Council Brain Network Dynamics Unit, University of Oxford, United Kingdom

13 <sup>4</sup>Department of Neuroscience and Biomedical Engineering, Aalto University School of Science, Espoo, Finland

14 <sup>5</sup>Neurocenter, Helsinki University Hospital and Clinical Neurosciences, Neurology, University of Helsinki,  
15 Helsinki, Finland

16 <sup>6</sup>Wellcome Centre for Human Neuroimaging, Department of Imaging Neuroscience, UCL Queen Square Institute  
17 of Neurology, United Kingdom

18 <sup>7</sup>Centre for Human Brain Health, School of Psychology, University of Birmingham, Birmingham, United  
19 Kingdom

20 <sup>8</sup>Department of Neurology, Helsinki University Hospital and Clinical Neurosciences, Neurology, University of  
21 Helsinki, Helsinki, Finland

22

23 Corresponding author:

24 Dr Catharina Zich

25 [c.zich@ucl.ac.uk](mailto:c.zich@ucl.ac.uk); [catharina.zich@ndcn.ox.ac.uk](mailto:catharina.zich@ndcn.ox.ac.uk)

26 Department of Clinical and Movement Neurosciences

27 UCL Queen Square Institute of Neurology

28 33 Queen Square, 3rd floor, Box 146

29 London WC1N 3BG

30

31 Keywords (max 6)

32 Acute stroke, Connectivity, MEG, MRI, Sensorimotor system, Tactile stimulation

## 33 **Abstract**

34 Improving outcomes after stroke depends on understanding both the causes of initial  
35 function/impairment and the mechanisms of recovery. Recovery in patients with initially low  
36 function/high impairment is variable, suggesting the factors relating to initial  
37 function/impairment are different to the factors important for subsequent recovery. Here we  
38 aimed to determine the contribution of altered brain structure and function to initial severity  
39 and subsequent recovery of the upper limb post-stroke.

40 The Nine-Hole Peg Test was recorded in week 1 and one-month post-stroke and used to divide  
41 36 stroke patients (18 females, age: M = 66.56 years) into those with high/low initial function  
42 and high/low subsequent recovery. We determined differences in week 1 brain structure  
43 (Magnetic Resonance Imaging) and function (Magnetoencephalography, tactile stimulation)  
44 between high/low patients for both initial function and subsequent recovery. Lastly, we  
45 examined the relative contribution of changes in brain structure and function to recovery in  
46 patients with low levels of initial function.

47 Low initial function and low subsequent recovery are related to lower sensorimotor  $\beta$  power  
48 and greater lesion-induced disconnection of contralateral [ipsilesional] white-matter motor  
49 projection connections. Moreover, differences in intra-hemispheric connectivity (structural and  
50 functional) are unique to initial motor function, while differences in inter-hemispheric  
51 connectivity (structural and functional) are unique to subsequent motor recovery.

52 Function-related and recovery-related differences in brain function and structure after stroke  
53 are related, yet not identical. Separating out the factors that contribute to each process is key to  
54 identifying potential therapeutic targets for improving outcomes.

55

## 56 **Keywords**

57 Acute stroke, Brain function, Brain structure, Motor function, Motor recovery

## 58 **1. Introduction**

59 Stroke is a leading cause of disability worldwide. One in four people will have a stroke in their  
60 lifetime, and a quarter of those survivors remain moderately to severely disabled ten years later.  
61 Upper limb motor impairment is a common consequence of stroke that can limit activities of  
62 daily living and impact quality of life (Broeks et al., 1999).

63  
64 Improving outcomes for stroke survivors will require an understanding of the mechanisms that  
65 support recovery. It is important to make the distinction between outcome and recovery.  
66 Outcome reflects the level of function/impairment at a given time post-stroke and is partially  
67 related to initial function/impairment. Recovery is a dynamic process defined as a return to or  
68 towards premorbid behavioural levels (Levin et al., 2009; Rothi & Horner, 1983). The fact that  
69 people with the same initial function/impairment can have different recovery profiles  
70 (Prabhakaran et al., 2008; Winters et al., 2015; Zarahn et al., 2011) indicates that the factors  
71 important for outcome and for subsequent recovery may be quite different (Ward, 2017).  
72 Identifying biomarkers of post-stroke recovery requires us to disentangle initial  
73 function/impairment-related and recovery-related differences in post-stroke brain function and  
74 structure. Functional and structural human neuroimaging provide complementary information  
75 to clinical measures (Laaksonen et al., 2012; Roiha et al., 2011; Ward, Brown, et al., 2006;  
76 Ward et al., 2003a) and can thus advance our understanding of recovery (Ward et al., 2003b,  
77 2004; Ward, Newton, et al., 2006).

78  
79 Previous investigations of the prognostic value of post-stroke brain structure have used lesion  
80 size, as well as the lesion's direct and indirect effects on grey matter and white matter  
81 connections (Griffis et al., 2019, 2021; Rudrauf et al., 2008; Talozzi et al., 2023). Initial motor  
82 function/impairment and subsequent motor recovery show no or only weak relationships with  
83 lesion size (Alexander et al., 2010; C.-L. Chen et al., 2000; Egger et al., 2021; Zhu et al., 2010),  
84 but damage to key grey matter regions or white matter connections represent promising  
85 structural correlates of both initial motor function/impairment and subsequent motor recovery.  
86 The prognostic focus has largely been on the integrity of descending white matter projection  
87 connections, particularly the corticospinal tract (CST). CST integrity is related to post-stroke  
88 initial motor function/impairment (Maraka et al., 2014; Schulz et al., 2012; Swayne et al., 2008;  
89 Talelli et al., 2006) but can also account for differences in subsequent motor recovery  
90 independent of initial motor function/impairment (Byblow et al., 2015; Puig et al., 2017;

91 Rapisarda et al., 1996; Stinear et al., 2007). Here we ask whether in addition to CST integrity,  
92 other structural connections (projection, commissural and association connections) are related  
93 to either initial motor function and/or subsequent motor recovery (Rondina et al., 2016, 2017).  
94  
95 Structural brain imaging cannot fully account for variability in either initial  
96 function/impairment or subsequent recovery. The additional prognostic relevance of brain  
97 function therefore becomes important, particularly those measures reflecting the early post-  
98 stroke balance between cortical inhibition and excitation that strongly influences the potential  
99 for experience dependent plasticity (Carmichael, 2012; Clarkson et al., 2010; Ward, 2017).  
100 Here we investigate the contribution of sensorimotor beta activity ( $\beta$ , ~13-30Hz), which plays  
101 a vital role in the physiology and pathology of human movement and movement disorders. In  
102 fact, every movement is accompanied by a decrease in sensorimotor  $\beta$  activity (Event-Related  
103 Desynchronisation, suppression), which has been related to the activation of the sensorimotor  
104 cortex. The  $\beta$  suppression is followed by an increase in sensorimotor  $\beta$  activity (Event-Related  
105 Synchronisation, rebound), which has been related to active inhibition or the removal of  
106 excitation in the sensorimotor cortex (R. Chen & Hallett, 1999; Franzkowiak et al., 2010;  
107 Pfurtscheller, 1992; Salmelin et al., 1995). The  $\beta$  suppression-rebound complex is a robust  
108 phenomenon with high reproducibility (Espenhahn et al., 2017; Illman et al., 2021). Compared  
109 to healthy controls, stroke patients with upper limb impairments exhibit significantly lower  $\beta$   
110 rebound in the acute and chronic phase providing a potential biomarker for motor  
111 function/impairment post stroke (Espenhahn et al., 2020; Laaksonen et al., 2012; Parkkonen et  
112 al., 2017, 2018; Tang et al., 2020). Changes in the  $\beta$  suppression-rebound complex during  
113 motor learning (Alayrangues et al., 2019; Haar & Faisal, 2020; Tan et al., 2014, 2016;  
114 Torrecillos et al., 2018) further strengthen the link between sensorimotor  $\beta$  activity and the  
115 experience dependent plasticity on which motor learning is based. Mechanistically, animal  
116 (Yamawaki et al., 2008) and human (Hall et al., 2010; Jensen et al., 2005) studies demonstrated  
117 that  $\beta$  activity is mediated by inhibitory interneuron drive via GABA-A receptors. Therefore,  
118 we focused on sensorimotor  $\beta$  activity assessed very early post-stroke (within 1 week) as a  
119 marker of the potential for experience dependent plasticity. We used tactile stimulation, which  
120 increases to  $\beta$  activity in the primary motor cortex (M1) and the primary and secondary sensory  
121 cortex (S1, S2), unconfounded by residual movement. In addition to M1 and S1, area S2 is of  
122 particular interest because of its anatomical connections to S1 and its functional role as an  
123 integration hub (Disbrow et al., 2003; Hinkley et al., 2007; Inoue et al., 2002; Krubitzer &  
124 Kaas, 1990; Lewis & Van Essen, 2000). Building upon previous work suggesting that

125 modulatory afferent input may reach M1 via S2 (Laaksonen et al., 2012) we analyse the  
126 functional connectivity pattern of the three nodes: M1, S1, and S2.

127

128 Here we will address the following question: What are the key stroke-related changes in brain  
129 structure and brain function that are related to initial motor function and to subsequent motor  
130 recovery? We will then determine whether the process of recovery of motor function after  
131 stroke (independent of initial motor function) relies more on brain structure, brain function or  
132 both. Separating out the factors that contribute to initial motor function and those that are  
133 related to the subsequent motor recovery process itself is key to identifying potential  
134 therapeutic targets for promoting post-stroke motor recovery.

## 135 **2. Materials and methods**

136 Collecting high-quality neuroimaging data in acute stroke patients is extremely challenging, so  
137 here we capitalise on existing high-quality data. Data from two previously published articles,  
138 i.e. dataset 1 (Laaksonen et al., 2012) and dataset 2 (Parkkonen et al., 2018), were combined.  
139 Participants were recruited using the same inclusion and exclusion criteria, data were acquired  
140 in the same institute, and comparable experimental designs were used. We here conduct  
141 entirely new analyses to quantify post-stroke structural connectivity and functional  
142 connectivity between sensorimotor areas at the source level.

143

### 144 **2.1 Experimental design**

#### 145 **2.1.1 Ethical approval**

146 For both studies, the Local Ethics Committee of the Helsinki and Uusimaa Hospital District  
147 approved the study protocol, and all subjects provided written informed consent.

148

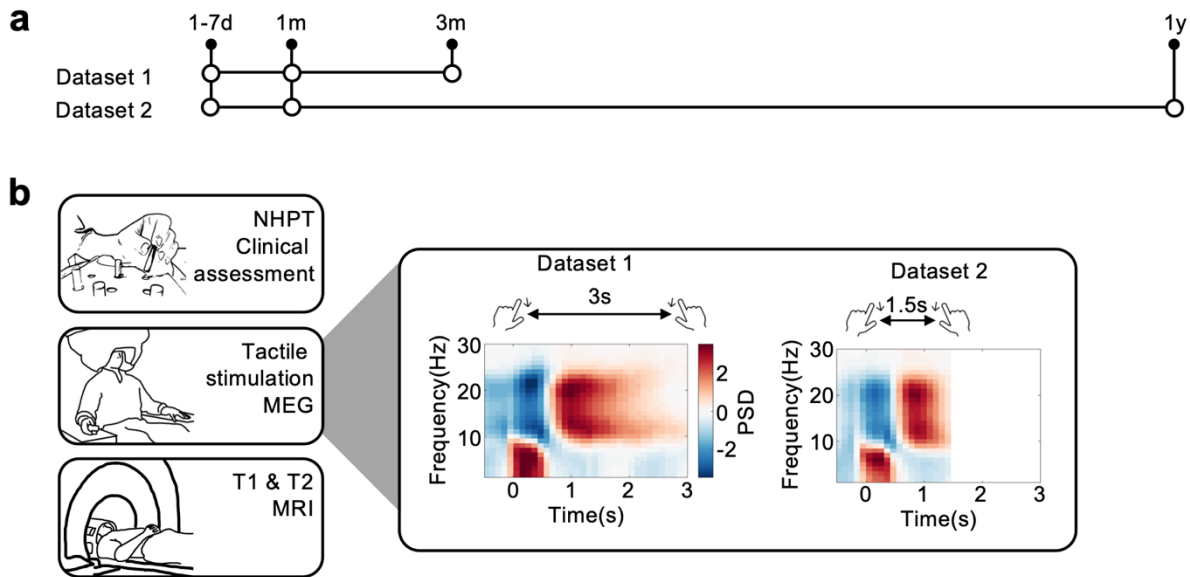
#### 149 **2.1.2 Subjects**

150 Patients with first-ever stroke in the middle cerebral artery territory causing unilateral upper  
151 limb impairments were recruited from the Department of Neurology, Helsinki University  
152 Hospital. Exclusion criteria were earlier neurological diseases, mental disorders, neurosurgical  
153 operations or head traumas, unstable cardiovascular/general condition. Eleven of the 18  
154 patients used in (Laaksonen et al., 2012) were included, as 7 MRI scans were not available.  
155 From the 27 patients in (Parkkonen et al., 2018), 25 patients were used for this analysis, as 2  
156 MRI scans were not available. Here we only include patients with MRI and MEG scans, thus,  
157 the total sample comprises 36 patients (18 females, age:  $M = 66.56$ ;  $SD = 8.52$ ; range 45-84  
158 years; see **SI Table 1**).

159

#### 160 **2.1.3 Time points and measurements**

161 Data were recorded at three time points (**Fig. 1a**). For dataset 1 (Laaksonen et al., 2012), these  
162 time points are 1-7 days ( $T_0$ ), 1 month ( $T_1$ ), and 3 months ( $T_2$ ) post-stroke. For dataset 2  
163 (Parkkonen et al., 2018), these time points are 1-7 days ( $T_0$ ), 1 month ( $T_1$ ), and 12 months ( $T_2$ )  
164 post-stroke. Here we focus on the clinical data, MEG data and MRI data from  $T_0$  and use the  
165 clinical data from  $T_1$  for recovery-related analysis.



166

167

### Fig. 1. Study design.

168 a) Timeline for dataset 1 (Laaksonen et al., 2012) and dataset 2 (Parkkonen et al., 2018), both comprising three  
169 assessment time points.

170 b) Details of each assessment time point. Each assessment time point comprises a clinical assessment (NHPT)  
171 and MEG scan. In addition, a MRI scan was conducted at the first two assessment time points. MEG data were  
172 collected during tactile stimulation of the index finger. The interstimulus interval was 1.5s for dataset 2 and 3s  
173 for dataset 1. Power spectral density (PSD) is shown. In both datasets, clear  $\beta$  (13-30Hz) suppression (blue) and  
174 rebound (red) can be seen.

175

## 176 2.2 Clinical data

177 A series of clinical measures were obtained, see (Laaksonen et al., 2012; Parkkonen et al.,  
178 2018). Here we focus on manual dexterity quantified by the Nine-Hole Peg Test (NHPT). The  
179 NHPT demands well-functioning motor and somatosensory systems, as well as a fluent  
180 integration between these two. Therefore, it serves well as a clinical measure of upper limb  
181 motor function. Specifically, NHPT performance is quantified by the time taken to remove and  
182 replace nine pegs into nine holes, with a maximum time of 120 seconds in dataset 2 (Parkkonen  
183 et al., 2018), and 180 seconds in dataset 1 (Laaksonen et al., 2012). Based on the initial NHPT  
184 performance patients were grouped into low function patients (did not complete NHPT within  
185 120 seconds) and high function patients (completed NHPT within 120 seconds, see Fig. 2a).  
186 Further, patients were grouped into patients who improved (difference between NHPT at  $T_1$   
187 and  $T_0 < 0$ ) and patients who didn't improve (difference between NHPT at  $T_1$  and  $T_0 = 0$ , see  
188 Fig. 5a).

189

## 190 2.3 MEG data

### 191 2.3.1 MEG data acquisition

192 MEG data were acquired using a whole-scalp 306-channel MEG system (204 planar  
193 gradiometers and 102 magnetometers; Vectorview™; Elekta Oy, Helsinki, Finland). Data were  
194 sampled at 944.8Hz with a band-pass filter of 0.03-308Hz in dataset 1 (Laaksonen et al., 2012),  
195 and at 1001.6Hz with a band-pass filter of 0.03-330Hz in dataset 2 (Parkkonen et al., 2018).  
196 Eye movements were simultaneously recorded via vertical electro-oculogram. Head position  
197 was recorded with respect to the MEG sensors using four head-position (HPI) coils. The  
198 locations of HPI coils, three anatomical fiducials (the nasion and two preauricular points) and  
199 head shape points (number of head shape points:  $M = 35.68$ ;  $SD = 15.71$ ; range = 11-61) were  
200 digitized using a 3D tracking system to allow alignment of the MEG and MRI coordinate  
201 system. Data were recorded according to the clinical condition of the patients, either in a sitting  
202 or supine position. A nurse inside the magnetically shielded room observed the patients for any  
203 possible movements.

204

### 205 **2.3.2 Tactile stimulation**

206 MEG data were collected during tactile stimulation of the index finger. Tactile stimulation  
207 reliably induces a sensorimotor  $\beta$  suppression-rebound complex in healthy controls and stroke  
208 patients (Bardouille et al., 2010; Gaetz & Cheyne, 2006). Importantly, tactile stimulation  
209 targets purely tactile fibres and avoids inter- and intra-individual differences in movement  
210 ability, allowing direct cross-sectional and longitudinal comparisons.

211 Pneumatic diaphragms driven by compressed air were used to deliver tactile stimuli to the tip  
212 of the index finger. Stimuli were alternately delivered to both index fingers with an  
213 interstimulus interval of 3005ms in dataset 1 (Laaksonen et al., 2012) or 1500ms in dataset 2  
214 (Parkkonen et al., 2018) (**Fig. 1b**). 60–80 stimuli were applied to each hand. The same stimulus  
215 intensity was applied to all subjects.

216

### 217 **2.3.3 MEG data pre-processing**

218 A summary of the data processing pipeline is shown in **SI Fig. 1**. External noise was reduced  
219 from MEG data using the MNE-Python (version 0.22.0) implementation of temporal signal-  
220 space separation (tSSS)/Maxwell filtering. MEG pre-processing was performed using the  
221 Oxford Centre for Human Brain Activity (OHBA) Software Library (OSL, [https://ohba-  
222 analysis.github.io/osl-docs/](https://ohba-analysis.github.io/osl-docs/)) version 2.2.0 using Matlab2022a. OSL builds upon Fieldtrip,  
223 SPM and FSL to provide a range of useful tools for M/EEG analyses. Continuous data were  
224 down-sampled to 250Hz and a band-pass filtered (1-45Hz). Time segments containing artefacts



225 were identified using the generalised extreme studentized deviate method (GESD)(Rosner,  
226 1983) on the standard deviation of the signal across all sensors in 1s non-overlapping windows,  
227 with a maximum number of outliers limited to 20% of the data and adopting a significance  
228 level of 0.05. Data segments identified as outliers were excluded from subsequent analyses.  
229 Further, denoising was conducted via independent component analysis (ICA) using temporal  
230 FastICA across the sensors (Hyvarinen, 1999). 62 independent components were estimated and  
231 components representing stereotypical artefacts such as eye blinks, eye movements, and  
232 electrical heartbeat activity were manually identified and regressed out of the data.  
233 Magnetometers and Planar-Gradiometers were normalised by computing the eigenvalue  
234 decomposition across sensors within each coil type and dividing the data by the smallest  
235 eigenvalue within each (Woolrich et al., 2011). Data were segmented from -0.5s to 1.5s or 3s  
236 depending on the interstimulus interval. Only trials with tactile stimulation of the affected hand  
237 were considered for this analysis. Registration between structural MRI and the MEG data was  
238 performed with RHINO (Registration of head shapes Including Nose in OSL), which makes  
239 an initial registration between the anatomical and polhemous fiducial landmarks. This fit is  
240 refined using an Iterative closest point (ICP) algorithm to optimise the correspondence between  
241 the polhemous headshape points and the mesh of the scalp extracted from the structural MRI.  
242 A single shell forward model was constructed using the individual inner skull mesh extracted  
243 from the structural MRI. Segmented data were projected onto an 8 mm grid in source space  
244 using a Linearly Constrained Minimum Variance (LCMV) vector beamformer (Van Veen &  
245 Buckley, 1988; Woolrich et al., 2011). Six regions of interest (ROIs) were considered: left and  
246 right M1, S1, and S2, as defined by the modified Schaefer Yeo parcellation ((Yeo et al., 2011),  
247 available from the *Lesion Quantification Toolkit*  
248 <https://wustl.app.box.com/v/LesionQuantificationToolkit>, (Griffis et al., 2021)). A single time  
249 course was estimated per ROI from the first principal component across the voxels within an  
250 ROI. Spatial leakage was attenuated using a symmetric multivariate leakage correction  
251 (Colclough et al., 2015, 2016).

252

### 253 **2.3.4 Functional Connectivity**

254 MEG features were extracted in Python (version 3.9.9) with core dependencies as numpy  
255 (Harris et al., 2020) and scipy (Virtanen et al., 2020) using the Spectral Analysis In Linear  
256 Systems toolbox (Quinn & Hymers, 2020).

257 Linear dependencies between the six ROI time-series  $X$  were modelled using a multivariate  
258 autoregressive (MVAR) model of order  $p = 6$  following the procedures outlined in (Quinn et  
259 al., 2021). For a review of these methods see (Blinowska, 2011).

260

$$261 \quad X(t) = \sum_{k=1}^p A_k X(t-k) + \epsilon(t)$$

262

263 The autoregressive parameters  $A$  are transformed into the frequency domain using the Fourier  
264 transform:

265

$$266 \quad A(f) = \sum_{k=1}^p A_k e^{-i2\pi ft}$$

267

268 The spectral matrix  $S(f)$  is computed from  $A(f)$  and the residual covariate matrix  $\Sigma$  The spectral  
269 matrix contains the power spectra of each region on the diagonal and the cross spectral densities  
270 on the off-diagonal elements.

271

$$272 \quad H(f) = (I - A(f))^{-1}$$

$$273 \quad S(f) = H(f)\Sigma H(f)^{-1}$$

274

275 The spectral matrix is used to compute the power spectral density  $PSD(f) = S(f)/\text{sample rate}$   
276 and the magnitude squared coherence (MSC).

277

$$278 \quad MSC_{ij}(f) = \frac{|S_{ij}(f)|^2}{\sqrt{|S_{ii}(f)S_{jj}(f)|}}$$

279

280 The MSC represents the cross-spectral density between two ROIs as a ratio of the power within  
281 each ROI. Finally, the Partial directed coherence (PDC) (Baccalá & Sameshima, 2001) is  
282 computed from the Fourier transform of the autoregressive parameters.

283

$$284 \quad \bar{A}(f) = I - A(f)$$

$$285 \quad PDC_{ij}(f) = \frac{|\bar{A}_{ij}(f)|}{\sqrt{\sum_i |\bar{A}_{ij}(f)|^2}}$$

286

287 The PDC is closely related to the concept of Granger Causality. It ranges from zero to one and  
288 is normalised across columns of the inverse spectral matrix. The PDC at frequency  $f$  between  
289 signal  $i$  and  $j$  reflects the outflow of influence from  $i$  to  $j$  as a proportion of the total outflow  
290 from  $i$  to all nodes (Baccalá & Sameshima, 2001; Bastos & Schoffelen, 2016). In other words,  
291 if the PDC of the connection between  $i$  and  $j$  is large, it indicates that information in the recent  
292 past of time series  $i$  improves the prediction of the next step in time series  $j$  relative to how well  
293 the past of time series  $i$  improves prediction of all nodes.

294 In summary, PSD represents the strength of the beta activity within each ROI, whilst MSC  
295 represent the strength and PDC the direction of functional connectivity between ROIs. PSD,  
296 MSC, and PDC were baseline corrected (-0.5s to 0s) and subsequently averaged across the  $\beta$   
297 rebound time window (0.6s to 1.2s).

298

## 299 **2.4 MRI data**

### 300 **2.4.1 MRI data acquisition**

301 The MRI protocol was acquired using a 3T Philips Achieva MRI scanner (Philips Medical  
302 Systems, The Netherlands). A high-resolution 3D T1-weighted scan (T1 3D TFE SENSE, TR  
303 = 9.9 ms, TE = 4.6 ms, voxel size =  $0.88 \times 0.83 \times 0.83$  mm<sup>3</sup>, dimensions =  $187 \times 288 \times 288$   
304 slices, flip angle = 8 degrees, bandwidth = 149) and a 3D T2-weighted scan was acquired (T2  
305 TSE 4mm CLEAR, TR = 4000 ms, TE = 80 ms, voxel size =  $0.469 \times 0.469 \times 4.4$  mm<sup>3</sup>,  
306 dimensions =  $512 \times 512 \times 32$ , flip angle = 90 degrees, bandwidth = 216).

307

### 308 **2.4.2 Lesion mapping**

309 Stroke lesions were demarcated using the semi-automated segmentation algorithm *Clusterize*  
310 ([https://www.medizin.uni-tuebingen.de/de/das-](https://www.medizin.uni-tuebingen.de/de/das-klinikum/einrichtungen/kliniken/kinderklinik/kinderheilkunde-iii/forschung-iii/software)  
311 [klinikum/einrichtungen/kliniken/kinderklinik/kinderheilkunde-iii/forschung-iii/software](https://www.medizin.uni-tuebingen.de/de/das-klinikum/einrichtungen/kliniken/kinderklinik/kinderheilkunde-iii/forschung-iii/software))  
312 applied to the axial T2 image acquired at  $T_0$ . Agreement between a manual segmentation and  
313 the semi-automated lesion maps obtained with *Clusterize* has been shown to be excellent in  
314 acute stroke using CT, DWI and T2 FLAIR (de Haan et al., 2015; Ito et al., 2019; Wilke et al.,  
315 2011). The resulting lesions were manually verified and if necessary corrected. Lesion maps  
316 were smoothed using a 2 mm full-width half maximum (FWHM) Gaussian kernel. Lesions  
317 were normalised to standard MNI space and left hemispheric lesions were flipped.

318

### 319 **2.4.3 Lesion size and ROI damage**

320 To investigate if differences in initial motor function and subsequent recovery are due to lesion  
321 size or direct damage to M1, S1 or S2 cortex, we calculated the lesion size and the ROI damage  
322 for M1, S1, and S2 using *Lesion Quantification Toolkit*  
323 (<https://wustl.app.box.com/v/LesionQuantificationToolkit>)(Griffis et al., 2021). Specifically,  
324 ROI damage quantifies the overlap between the lesion and each ROI as a percent of voxels  
325 with the ROI that overlaps with the lesion. Despite some limitations (Seghier, 2023), ROI  
326 damage can provide a straightforward way of reducing the dimensionality of the lesion's effect  
327 on brain structure.

328

### 329 **2.4.4 Structural connectivity**

330 To characterise structural connections as well as the relationship between functional and  
331 structural connections, we quantified voxel-wise percent disconnection maps and the effect of  
332 the lesion on the relevant association, projection, and commissural connections, again using  
333 the *Lesion Quantification Toolkit* (Griffis et al., 2021).

334 The voxel-wise percent disconnection map indicates for each voxel the percentage of all the  
335 streamlines (computed from the HCP-842 streamline tractography atlas) in that voxel relative  
336 to those streamlines that are expected to be disconnected by the lesion (for more details see  
337 (Griffis et al., 2021)).

338 For projection connections and commissural connections, lesion-related damage to white  
339 matter tracts (i.e., tract disconnection) was quantified. Tract disconnection is the percent of  
340 streamlines of the HCP-842 population-average streamline tractography atlas that intersect the  
341 lesion (for more details see (Griffis et al., 2021)). While the atlas comprises 70 tracts here we  
342 focus on the motor projection connections (corticospinal tract [CST], corticostriatal pathway  
343 [CS], corticothalamic pathway [CT], frontopontine tract [FPT], parietopontine tract [PPT]) and  
344 motor commissural connections (mid-anterior corpus callosum, central corpus callosum, mid-  
345 posterior corpus callosum).

346 The structural connection between the cortical ROIs M1, S1, and S2, i.e., association  
347 connections, cannot simply be assessed using the 70 tracts of the HCP-842 population-average  
348 streamline tractography atlas. Therefore, these association connections were quantified using  
349 the structural shortest path lengths (SSPL) between M1, S1, and S2. SSPL reflects the  
350 minimum number of direct parcel-to-parcel (using the modified Schaefer Yeo parcellation  
351 ((Yeo et al., 2011)) white matter connections (computed from the HCP-842 streamline

352 tractography atlas) that must be traversed to establish a structural path between two ROIs (for  
353 more details see (Griffis et al., 2021)). Here we report the lesion-induced increases in SSPLs  
354 relative to the atlas SSPL matrix.

355

## 356 **2.5 Statistical analysis**

357 Null-hypothesis testing was carried out with non-parametric permutations (Maris &  
358 Oostenveld, 2007; Nichols & Holmes, 2002). Depending on the hypothesis test, different forms  
359 of non-parametric permutation are used, though the overall procedure is similar. To compare  
360 differences between subgroups row-shuffle permutation is used. To test whether a  
361 measurement deviates from zero sign-flipping permutation is used. A null distribution of the  
362 test statistic is derived by recomputing the test statistic after each permutation. The observed  
363 test statistic is then compared to this null distribution and is ‘significant’ if it exceeds a pre-set  
364 critical threshold. Here we build the null distribution from 5000 repetitions and use the 95<sup>th</sup>  
365 percentile (indicated with \*) and the 99<sup>th</sup> percentile (indicated with \*\*) of the null distribution  
366 as thresholds.

367 For prediction analysis forward stepwise linear regression was used to identify possible  
368 predictors of the outcome improvement status (improved = 0, didn’t improve = 1) as  
369 implemented in R (version 4.0.2). Predictors were standardised using z-transformation. At each  
370 step, predictors were included when  $p < 0.15$  (Wald test) and removed when  $p \geq 0.15$  (Wald  
371 test). Predictors showing high collinearity (variance inflation factor (VIF)  $> 2.5$ ) were re-  
372 assessed. A backward stepwise approach was used to test the stability of the model (inclusion  
373 criterion:  $p \geq 0.15$ ; removal criterion:  $p < 0.15$ ; Wald test). The Brier score and area under the  
374 curve (AUC) of the receiver operating characteristic curve (ROC) were used to quantify the  
375 goodness of fit of the logistic regression model. Finally, accuracy, sensitivity, specificity,  
376 positive predictive value (PPV), and negative predictive value (NPV), including the  
377 corresponding 95% CIs, were calculated using two-way contingency tables.

378

## 379 **2.6 Data availability**

380 We will consider requests to access the data in a trusted research environment as part of a  
381 collaboration if requirements of EU data protection and Finnish legislation on health data are  
382 followed. Contact: [nina.forss@hus.fi](mailto:nina.forss@hus.fi).

### 383 **3. Results**

#### 384 **3.1 Acute post-stroke brain function and structure relate to** 385 **initial motor function**

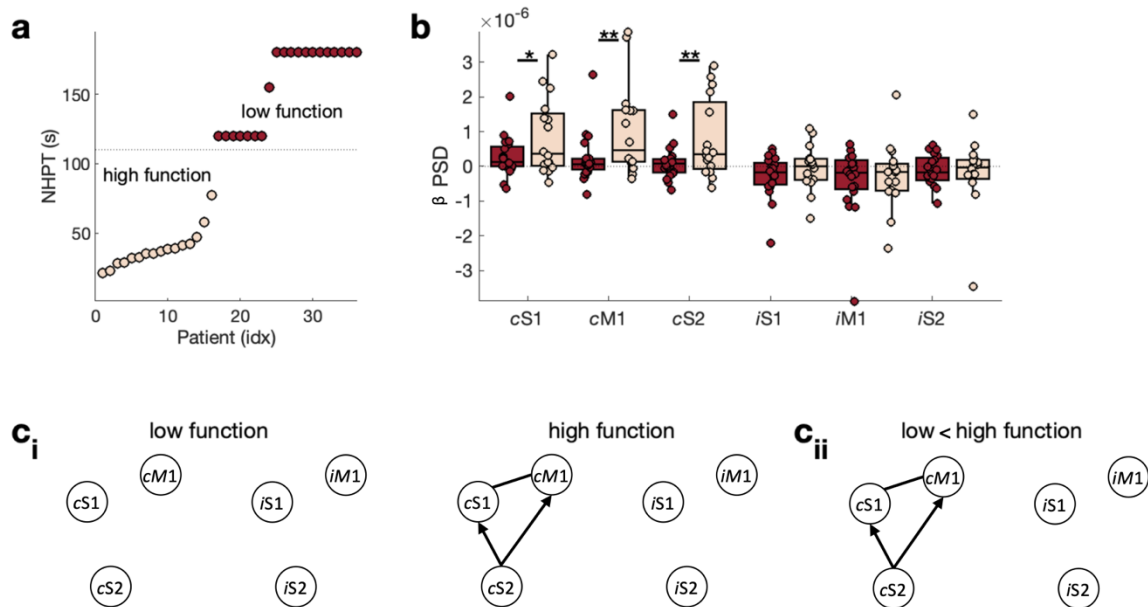
386 First, we assess motor function-related differences in brain function and structure in the acute  
387 phase post-stroke ( $T_0$ ). To this end, patients are grouped based on their initial NHPT scores  
388 into low and high function patients. Patients who could not complete the NHPT at  $T_0$  within  
389 120 seconds are referred to as low function patients (**Fig. 2a**;  $N = 20$ ; 11 females, age:  $M =$   
390  $67.85$ ;  $SD = 9.11$ ; range 47-84 years), while patients who could complete the NHPT within 120  
391 seconds are referred to as high function patients ( $N = 16$ ; 7 females, age:  $M = 64.94$ ;  $SD = 7.70$ ;  
392 range 45-76 years). Based on these definitions, patients fall into two distinct groups (**Fig. 2a**).  
393

##### 394 3.1.1 Brain function

395 We then asked if brain function differs between high and low function patients. Extending the  
396 previous reports on the MEG sensor level (Laaksonen et al., 2012; Parkkonen et al., 2018), we  
397 quantified the sensorimotor  $\beta$  rebound on source level from contralateral [ipsilesional] and  
398 ipsilateral [contralesional] sensorimotor ROIs (M1, S1, S2). In line with the sensor level  
399 analyses, we found that the sensorimotor  $\beta$  rebound was significantly reduced in the  
400 contralateral [ipsilesional] M1 ( $t(34)=-2.39, p<0.05$ ), S1 ( $t(34)=-2.10, p<0.01$ ), and S2 ( $t(34)=-$   
401  $2.48, p<0.01$ ) in initially low function patients when compared to high function patients (**Fig.**  
402 **2b**). No significant differences were observed for the homologous ipsilateral [contralesional]  
403 ROIs (all three  $p$ 's  $> 0.05$ ).  
404

405 To further understand the underlying mechanisms of these motor function-related differences  
406 in the sensorimotor  $\beta$  rebound, we next investigated the strength (i.e., Magnitude-Squared  
407 Coherence, MSC) and directionality (i.e., Partial Directed Coherence, PDC) of functional  
408 connectivity. Regarding intra-hemispheric functional connectivity strength, in low function  
409 patients none of the connections were strong enough to reach statistical significance (**Fig. 2ci**,  
410 **SI Fig. 2ai**). In contrast, in high function patients all contralateral [ipsilesional] intra-  
411 hemispheric functional connections were strong enough to pass the significance threshold (S1-  
412 M1 [ $t(15)=2.73, p<0.01$ ], S2-S1 [ $t(15)=2.04, p<0.05$ ], S2-M1 [ $t(15)=2.57, p<0.01$ ]), resulting  
413 in significant differences in functional connectivity strengths between high and low function  
414 patients (all three  $p$ 's  $< 0.05$ , **Fig. 2cii**, **SI Fig. 2aii**). Inter-hemispheric connections were not

415 significant in either patient group. Analysing the directionality of functional connectivity  
 416 showed no significant directionality (i.e., none of the connections showed a directionality that  
 417 was significantly different from zero) in low function patients. In contrast, in high function  
 418 patients contralateral [ipsilesional] S2-M1 ( $t(15)=-2.34$ ,  $p<0.05$ ) and S2-S1 ( $t(15)=-3.45$ ,  
 419  $p<0.01$ ), were driven by S2 (**Fig. 2c<sub>i</sub>**, **SI Fig. 2b<sub>i</sub>**), and the directionality of these functional  
 420 connections differs significantly between the high and low function patients (both  $p$ 's<0.05,  
 421 **Fig. 2c<sub>ii</sub>**, **SI Fig. 2b<sub>i</sub>**).



422

423 **Fig. 2. Behaviour and brain function for low and high function patients.**

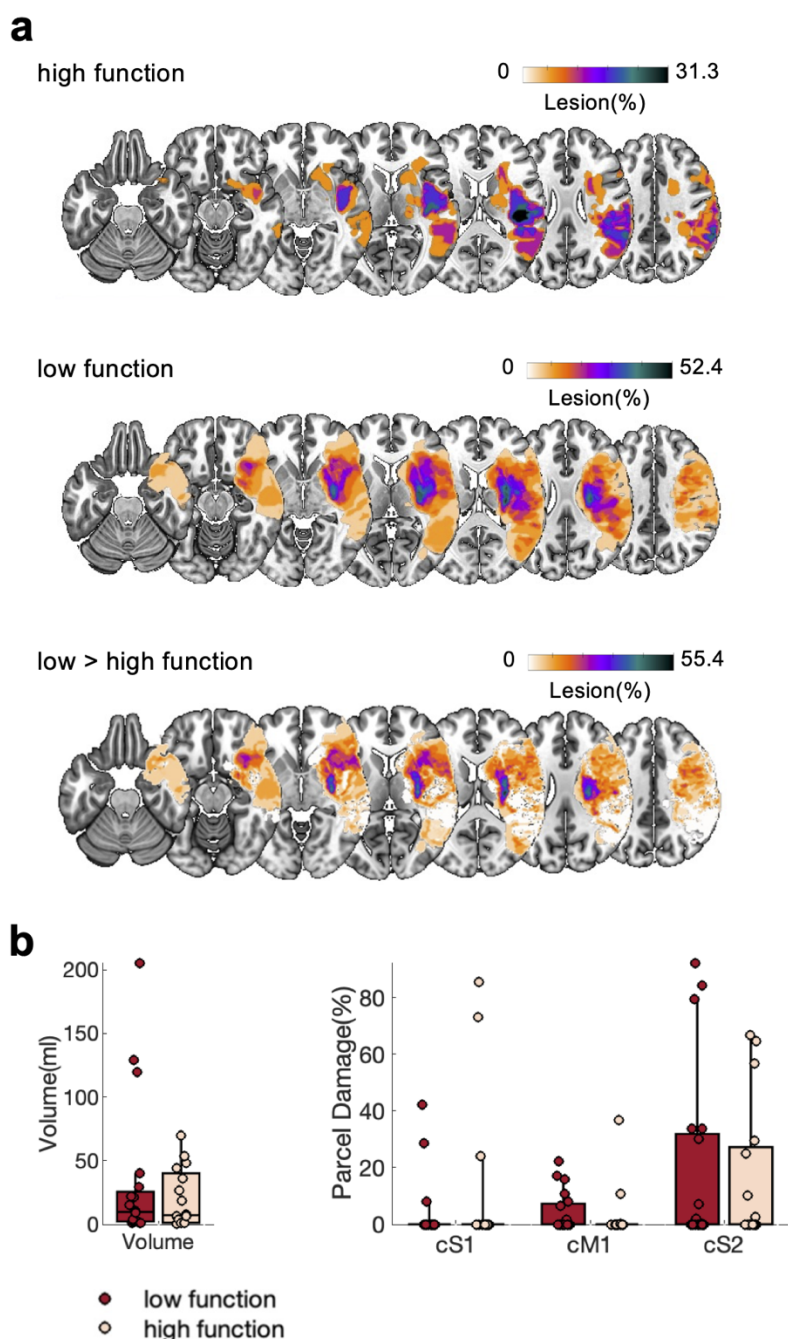
424 a) Patients are grouped into high function and low function patients based on their NHPT performance at  $T_0$ .  
 425 b) Power (PSD) in the  $\beta$  frequency range (13-30Hz) during the  $\beta$  rebound for contralateral [ipsilesional] 'c' and  
 426 ipsilateral [contralesional] 'i' M1, S1, and S2.  
 427 c<sub>i</sub>) Connectivity strength and direction for low function (left) and high function (right) patients. Connections  
 428 whose strength is significantly different from zero are highlighted by a solid line. Connections whose directionality  
 429 is significantly different from zero have an arrow indicating the directionality.  
 430 c<sub>ii</sub>) Difference in connectivity strength and direction between low and high function patients.

431

### 432 3.1.2 Brain structure

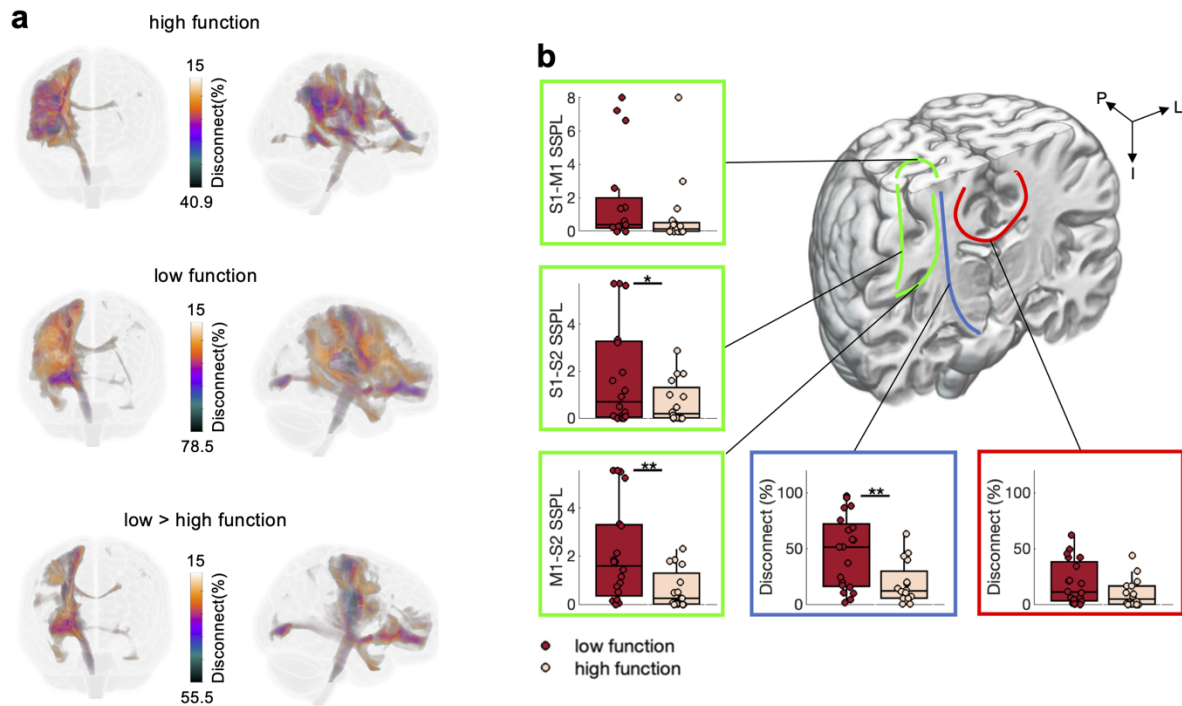
433 Next, we asked if brain structure differs between high and low function patients. Lesion  
 434 volume, as well as extent of M1, S1, and S2 damage, did not significantly differ between low  
 435 and high function patients (all  $p$ 's>0.05, **Fig. 3a,b**), indicating that the differences in initial  
 436 motor function patients are not simply explained by these direct lesion characteristics. We  
 437 complemented our functional connectivity analysis with structural connectivity analysis.  
 438 Descriptively, low function patients show higher overall tract disconnection than high function  
 439 patients (**Fig. 4a**). Statistically, we observed significant differences in the association  
 440 connections between S2-S1 ( $t(34)=1.85$ ,  $p<0.05$ ) and S2-M1 ( $t(34)=2.67$ ,  $p<0.01$ ), with longer

441 structural shortest path lengths (SSPLs), for low function patients (**Fig. 4b**). Similarly, motor  
 442 projection connections (i.e., CST, CS, CT, FPT, PPT) were significantly different between  
 443 groups ( $t(34)=3.04$ ,  $p<0.01$ , **Fig. 4b**, for individual tracts see **SI Fig. 3a**), with higher tract  
 444 disconnect for low function patients, while the inter-hemispheric commissural connections  
 445 (i.e., Mid Anterior, Central, Mid Posterior commissural connections) did not differ  
 446 significantly between low and high function patients ( $p>0.05$ , **Fig. 4b**, **SI Fig. 3b**).



447 **Fig. 3. Lesion maps, lesion volume, and S1, M1, S2 ROI damage for low and high function patients.**  
 448 *a) Heatmap of lesions for high function patients, low function patients, and the difference map between low and*  
 449 *high function patients. Left hemispheric lesions were flipped. Heatmaps are overlaid on an MNI template.*  
 450 *b) Lesion volume (left) and ROI damage for contralateral (ipsilesional) S1, M1, and S2.*  
 451





452 **Fig. 4. Structural connectivity for low and high function patients.**

453 a) Voxel-wise percent disconnection maps from the frontal and lateral view.

454 b) Association connections (green) quantified using structural shortest path lengths (SSPL) between M1, S1, and  
 455 S2. The average across motor projection connections (blue, see SI Fig. 3a for individual motor projection  
 456 connections) and the average across commissural motor connections (red, see SI Fig. 3b for individual  
 457 commissural motor connections). Note that the highlighted connections on the coronal slice are only schematic  
 458 representations. Significant differences between groups are highlighted ( $p < 0.05$  \*,  $p < 0.01$  \*\*).

460

461 To summarize, initial motor function, as quantified by the NHPT, is related to brain function  
 462 and brain structure. At the level of brain function, low initial motor function is related to a  
 463 lower  $\beta$  rebound in contralateral [ipsilesional] M1, S1, and S2, as well as lower functional  
 464 connectivity strength and directionality between these areas. At the level of brain structure, low  
 465 initial motor function is related to less direct association connections between these areas and  
 466 by higher disconnection of projection connections.

467

### 468 **3.2 Acute post-stroke brain function and structure relate to** 469 **subsequent motor recovery**

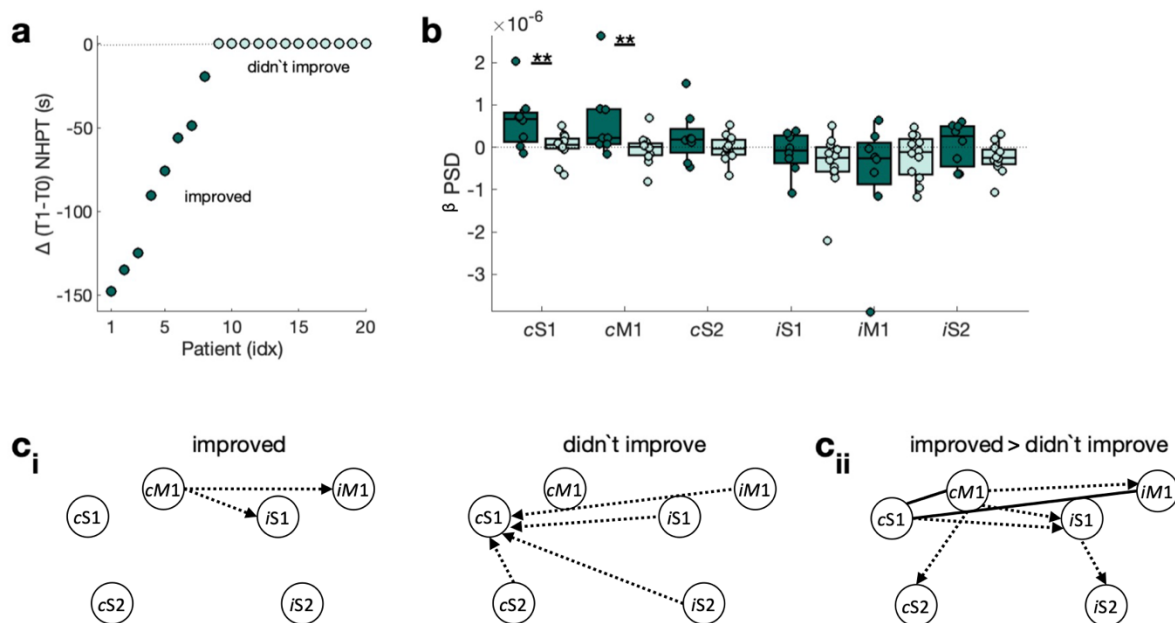
470 Next, we sought to explore whether brain function and structure in the acute stage ( $T_0$ ) can help  
 471 distinguish between patients who subsequently recover from patients who subsequently don't  
 472 recover ( $T_1$ ). As subsequent motor recovery is strongly related to initial motor  
 473 function/impairment (Prabhakaran et al., 2008; Winters et al., 2015) investigating purely  
 474 recovery-related processes requires careful correction for initial function/impairment or a  
 475 group of patients with similar initial function/impairment yet different subsequent recovery

476 trajectories. Here we focus on the group of initially low function patients, defined as those  
 477 patients who could not complete the NHPT at  $T_0$  within 120 seconds (**Fig. 2a**). These patients  
 478 were then divided based on the change in their NHPT performance (NHPT  $T_1 -$  NHPT  $T_0$ )  
 479 over 1 month, using  $< 0$  as the cut-off. Of the initially low function patients, eight patients  
 480 improved in the NHPT (3 females, age:  $M = 69.63$ ;  $SD = 9.21$ ; range 57-84 years), while twelve  
 481 patients didn't improve (8 females, age:  $M = 66.67$ ;  $SD = 9.25$ ; range 47-78 years) (**Fig. 5a**).

482

### 483 3.2.1 Brain function

484 First, we asked if brain function differs between patients who improved and patients who didn't  
 485 improve. Patients who improved from  $T_0$  to  $T_1$  have significantly higher sensorimotor  $\beta$   
 486 rebound in the contralateral [ipsilesional] M1 ( $t(18)=2.26, p<0.01$ ) and S1 ( $t(18)=2.77, p<0.01$ )  
 487 at  $T_0$  (**Fig. 5b**). Further, analysis of functional connectivity strength (i.e., MSC) showed no  
 488 significant connections in either group. Subsequent analysis of functional connectivity  
 489 direction (i.e., PDC) revealed that inter-hemispheric functional connectivity at  $T_0$  is driven by  
 490 the contralateral [ipsilesional] hemisphere in patients who improve from  $T_0$  to  $T_1$  (**Fig. 5ci, SI**  
 491 **Fig. 4bi, SI Results**), while patients who didn't improve from  $T_0$  to  $T_1$  exhibit the opposite  
 492 directionality (i.e., driven by the ipsilateral [contralesional] hemisphere, **Fig. 5ci, SI Fig. 4bi,**  
 493 **SI Results**), resulting in significant differences between patients who improve and patients  
 494 who didn't improve (**Fig. 5cii, SI Fig. 4bii, SI Results**).



495

496 **Fig. 5. Behaviour and brain function for patients who improved and patients who didn't improve considering**  
 497 **only patients who have initially low motor function.**

498 a) Patients are grouped into 'improved' and 'didn't improve' based on their difference in NHPT performance  
 499 (i.e.,  $T_1 - T_0$ ).

500 *b) Power (PSD) in the  $\beta$  frequency range (13-30Hz) during the  $\beta$  rebound for contralateral [ipsilesional] 'c' and*  
501 *ipsilateral [contralesional] 'i' M1, S1, and S2.*

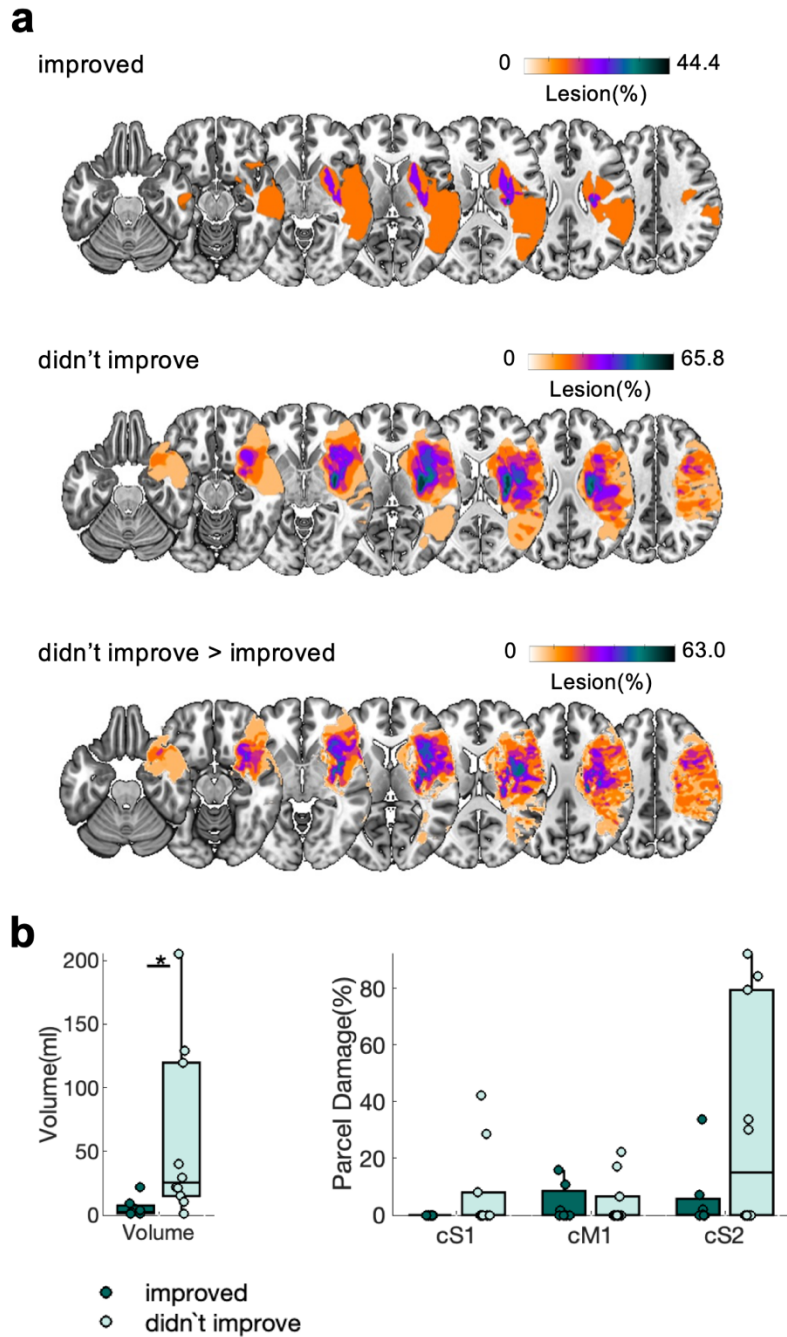
502 *ci) Connectivity strength and direction for patients who improve (left) and patients who didn't improve (right).*  
503 *Connections whose strength is significantly different from zero are highlighted by a solid line. Connections whose*  
504 *directionality is significantly different from zero have an arrow indicating the directionality. If only the direction,*  
505 *but not the strength is significant the connection is shown as a dashed line.*

506 *cii) Difference in connectivity strength and direction between patients who improve and patients who didn't*  
507 *improve.*

508

### 509 3.2.2 Brain structure

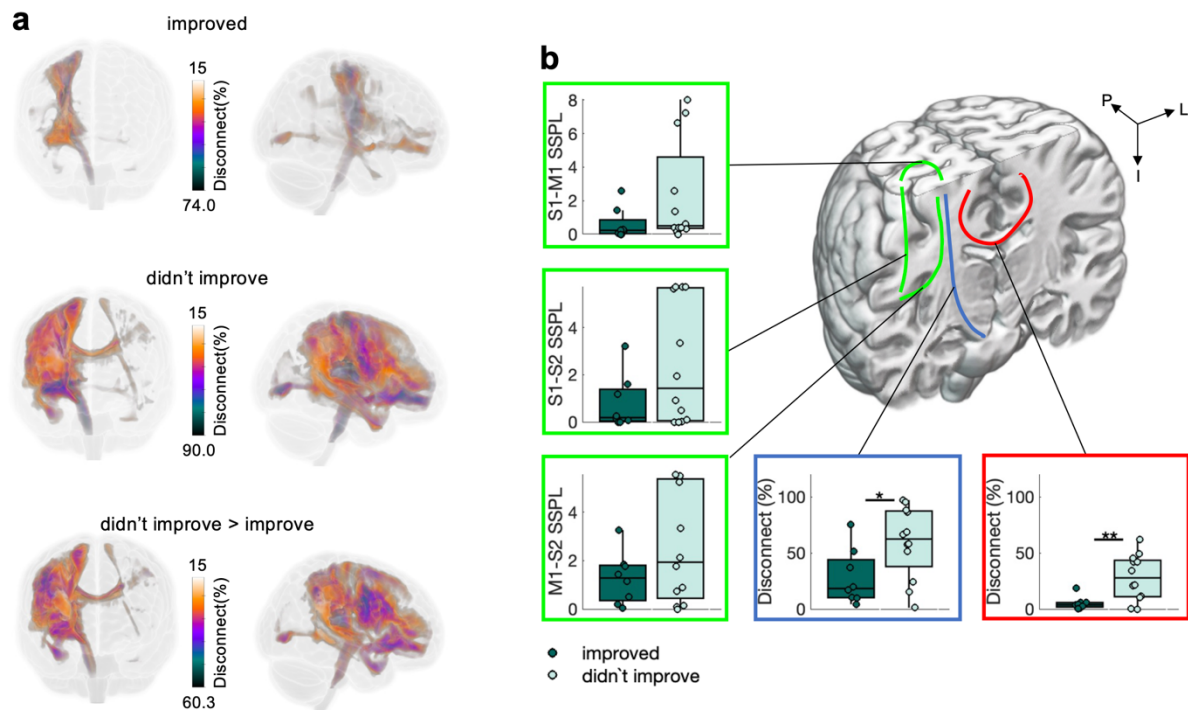
510 Next, we asked if brain structure differs between patients who improved and patients who  
511 didn't improve. Patients who didn't improve from T<sub>0</sub> to T<sub>1</sub> have larger lesions at T<sub>0</sub> ( $t(18)=2.01$ ,  
512  $p<0.05$ , **Fig. 6b**), but no significant differences in ROI damage were observed (all three  
513  $p's>0.05$ , **Fig. 6b**). Structural connectivity analysis further revealed no significant group  
514 differences for association connections between M1, S1, and S2 ( $p's>0.05$ , **Fig. 7b**) at T<sub>0</sub>.  
515 However, both, motor projection connections (i.e., CST, CS, CT, FPT, PPT,  $t(18)=-2.34$ ,  
516  $p<0.05$ , **Fig. 7b**, for individual tracts see **SI Fig. 5a**) and motor commissural connections (i.e.,  
517 Mid Anterior, Central, Mid Posterior commissural connections,  $t(18)=-3.08$ ,  $p<0.01$ , **Fig. 7b**,  
518 for individual tracts see **SI Fig. 5b**) at T<sub>0</sub>, were significantly different between groups (both  
519  $p's<0.01$ ), with higher tract disconnect for patients who didn't improve from T<sub>0</sub> to T<sub>1</sub>.



520

521 *Fig. 6. Lesion maps, lesion volume, and S1, M1, S2 ROI damage for patients who improved and patients who*  
522 *didn't improve considering only patients who have initially low motor function.*

523 *a, b) Same as Fig. 3.  $p < 0.05$  \*.*



524

525 **Fig. 7. Structural connectivity for patients who improve and patients who didn't improve considering only**  
 526 **patients who have initially low motor function.**

527 *a, b) Same as Fig. 4. See SI Fig. 5a,b for more details.*

528

529 Together, subsequent motor recovery in patients with initially low motor function, as quantified  
 530 by improvement in the NHPT from T<sub>0</sub> to T<sub>1</sub>, relates to brain function and brain structure  
 531 acquired at T<sub>0</sub>. At the level of brain function, severely affected patients who improve motor  
 532 function show a stronger T<sub>0</sub>  $\beta$  rebound in contralateral [ipsilesional] M1 and S1, and T<sub>0</sub> inter-  
 533 hemispheric connectivity driven by the contralateral [ipsilesional] hemisphere. At the level of  
 534 brain structure, severely affected patients who improve motor function have smaller lesions  
 535 and more intact motor projection and motor commissural connections.

536

### 537 **3.3 Predicting subsequent motor recovery in stroke patients who** 538 **have initially low motor function using multimodal neuroimaging**

539 Finally, we explored the potential to predict subsequent motor recovery in stroke patients who  
 540 have initially low motor function using multimodal neuroimaging. We focus on stroke patients  
 541 who have initially low motor function as initial motor function/impairment alone is insufficient  
 542 to reliably predict subsequent recovery in this subsample of patients (Prabhakaran et al., 2008;  
 543 Winters et al., 2015). To avoid overfitting, we focussed on the brain functional and structural  
 544 properties at T<sub>0</sub> which showed a significant difference between initially low function patients  
 545 who improved and initially low function patients who didn't improve from T<sub>0</sub> to T<sub>1</sub> (see Section

546 3.2). To recap, at the level of brain function these properties are M1  $\beta$  rebound (see **Fig. 5b**),  
547 S1  $\beta$  rebound (see **Fig. 5b**), strength of intra-hemispheric S1-M1 connectivity (MSC) (see **Fig.**  
548 **5c<sub>ii</sub>**), and strength of inter-hemispheric S1-M1 connectivity (MSC) (see **Fig. 5c<sub>ii</sub>**). At the level  
549 of brain structure these properties are lesion size (see **Fig. 6b**), motor projection connections  
550 (see **Fig. 7b**), and motor commissural connections (see **Fig. 7b**).

551 From these candidate variables measured at  $T_0$ , leave-one-out cross-validation and a forward  
552 stepwise logistic regression were used to identify possible predictors of subsequent motor  
553 recovery from  $T_0$  to  $T_1$ . Strong collinearity was found between M1 and S1  $\beta$  rebound, and so  
554 these variables were consequently averaged. The forward stepwise logistic regression reduced  
555 the significant predictors to (i) strength of inter-hemispheric S1-M1 connectivity (MSC) ( $\beta = -$   
556  $2.42$ , 95% CI =  $-4.76-0.10$ ,  $p = 0.042$ ) and (ii) integrity of motor projection connections ( $\beta =$   
557  $1.46$ , 95% CI =  $-0.18-3.09$ ,  $p = 0.080$ ). The Brier score (0.10) and the AUC of the ROC (0.92)  
558 suggest an excellent fit (for more model fit measures and alternative models see **SI Results**).  
559 Initially low function patients who had stronger functional inter-hemispheric S1-M1  
560 connectivity and more intact motor projection connections at  $T_0$  were likely to show subsequent  
561 motor recovery (**SI Fig. 6**). The accuracy of the model was 0.90 (95% CI = 0.68-0.99), the  
562 sensitivity 0.91 (95% CI = 0.62-0.99), and the specificity was 0.88 (95% CI = 0.47-0.99),  
563 whereas the PPV and NPV were, respectively, 0.92 (95% CI = 0.64-0.99) and 0.88 (95% CI =  
564 0.51-0.98). These results were confirmed by forward stepwise analysis.

## 565 **4. Discussion**

566 Here we asked what differences in acute post-stroke brain structure and function can account  
567 for differences in initial motor function and subsequent recovery of motor performance. To  
568 address these questions, we capitalised on hard-to-come-by high-quality MEG and MRI data  
569 collected in the first week post-stroke (Laaksonen et al., 2012; Parkkonen et al., 2018). We  
570 found that low initial motor function and low subsequent motor recovery are related to lower  
571 sensorimotor  $\beta$  rebound and greater lesion-induced disconnection of contralateral [ipsilesional]  
572 white-matter motor projection connections. Moreover, unique to initial motor function are  
573 differences in functional and structural intra-hemispheric connectivity, while differences in  
574 functional and structural inter-hemispheric connectivity are unique to subsequent motor  
575 recovery.

576

### 577 **4.1 $\beta$ rebound and projection connections as functional and** 578 **structural markers for initial motor function and subsequent** 579 **motor recovery**

580 In the first week post-stroke  $\beta$  rebound was lower (i) in low compared to high function patients;  
581 and (ii) in initially low function patients who improve motor function compared to patients  
582 who didn't improve motor function. This is in line with previous studies showing that  $\beta$   
583 rebound correlates with initial motor function/impairment (i.e., patients with lower  $\beta$  rebound  
584 show low function/high impairment) and subsequent motor recovery (i.e., patients with lower  
585  $\beta$  rebound show low subsequent recovery) (Laaksonen et al., 2012; Parkkonen et al., 2017,  
586 2018; Tang et al., 2020). Collectively these findings suggest that early post-stroke  $\beta$  rebound  
587 is a functional marker for initial motor function/impairment and subsequent motor recovery.

588 Overall, our MEG findings are in keeping with work in pre-clinical models of stroke that report  
589 early reduced neuronal activity in peri-infarct regions followed by restoration of activity (both  
590 peri-infarct and network connectivity) associated with recovery of function (see (Campos et  
591 al., 2023) for review). More specifically, lower  $\beta$  rebound is linked to lower GABA levels  
592 (Gaetz et al., 2011) and higher M1 cortical excitability (Hari et al., 1998; Salenius et al., 1997;  
593 Salmelin & Hari, 1994), so our results suggest that in the low function and poorer recovering  
594 patients, there is some very early motor cortex hyperexcitability, in keeping with previously  
595 observed reduced short interval cortical inhibition (SICI, related to GABA<sub>A</sub> signalling) and  
596 shlong interval cortical inhibition (LICI, related to GABA<sub>B</sub> signalling) in acute stroke. Several

597 techniques have been used to assess markers of cortical excitability after stroke in humans  
598 (Mäkelä et al., 2015; Motolese et al., 2023), which point to increased cortical excitability (or  
599 reduced inhibition) in the acute phase post stroke. This cortical hyperexcitability has often been  
600 highlighted as something that supports recovery (in animal models) by enhancing the potential  
601 for experience-dependent plasticity (Carmichael, 2012; Ward, 2017), but in our patients,  
602 cortical hyperexcitability does not appear to be beneficial.

603 The explanation for this might come in the changes in brain structure, where we demonstrated  
604 that, like  $\beta$  rebound, higher disconnection of several white matter projection connections is  
605 related to low initial motor function and low subsequent motor recovery. One idea is that the  
606 observed changes in cortical excitability (and by extension enhanced plasticity) cannot exert  
607 beneficial effects over motor recovery because of the disconnection of projections to spinal  
608 cord motoneurons or contralesional hemisphere. This hypothesis will need to be addressed in  
609 future studies.

610

## 611 **4.2 Cortical intra-hemispheric connectivity differs as a function** 612 **of initial motor function**

613 To further understand the function- and recovery-related reduction in the sensorimotor  $\beta$   
614 rebound we asked if intra- and inter-hemispheric differences in functional and structural  
615 connectivity relate to initial motor function and subsequent motor recovery. Intra-  
616 hemispherically, we observed function-related, but not recovery-related, differences in  
617 functional and structural connectivity between primary and secondary somatosensory areas and  
618 between motor and somatosensory areas. Specifically, we found that the ipsilesional M1-S1  
619 connection was stronger in high function patients and patients who recovered. In line with  
620 previous work, we found no clear directionality between M1 and S1 (Gandolla et al., 2021).  
621 While some studies provide clear evidence for M1 influencing S1, for example, the neural  
622 activity in somatosensory areas is modified by motor tasks (Ageranioti-Bélanger & Chapman,  
623 1992) or evidence from animal studies suggests that M1 provides weak input to nearly all  
624 pyramidal neurons in S1 (Kinnischtzke et al., 2016). Other studies showed that input to S1  
625 influences M1. For example, sensory stimulation facilitates functional reorganization of M1  
626 (Garry et al., 2005; Hamdy et al., 1998; Ridding & Ziemann, 2010), Transcranial Magnetic  
627 Stimulation over S1 increases M1 excitability in healthy individuals (de Freitas Zanona et al.,  
628 2023) and motor learning post-stroke (Brodie et al., 2014), and animal data suggest that S1  
629 input to M1 pyramidal cells can drive postsynaptic activity (Petrof et al., 2015). Together, it



630 seems that ipsilesional M1-S1 are strongly and reciprocally connected to ensure precise  
631 movements, and deficits in this connection are related to low motor function.

632

633 Regarding the connections between M1 and S2 as well as S1 and S2, we observed structurally  
634 a longer path length for low function patients than for high function patients, indicating that  
635 lesions disrupted the shortest path in low function patients. In addition, on the functional level,  
636 we found significant strength and directionality in functional connectivity in high function  
637 patients, with M1 and S1 both being driven by S2, whereas in low function patients no  
638 functional connectivity was found between these areas. S2 is the first cortical area that unites  
639 sensory information from the two body halves, thus it has been thought to be an important area  
640 for sensorimotor integration (Hinkley et al., 2007; Inoue et al., 2002) and bimanual tasks  
641 (Disbrow et al., 2001). This explains its dense connection with several areas in the parietal and  
642 frontal cortex, such as the posterior parietal and premotor areas (Disbrow et al., 2003; Krubitzer  
643 & Kaas, 1990; Lewis & Van Essen, 2000). Here, we observed a directionality whereby S2 was  
644 the leading area. This might be unexpected, given that both, S2 and S1, receive direct input  
645 from the ventroposterior thalamus (for review see (Jones, 1985), (Disbrow et al., 2002;  
646 Friedman & Murray, 1986)), which informed the theory that cortical somatosensory processing  
647 depends on hierarchically equivalent and parallel processing in S1 and S2 (Mountcastle, 1978,  
648 1986; Rowe et al., 1996). The directionality of the interaction between S1 and S2 has been  
649 probed using selective inactivation in marmosets, revealing that ~70% of S2 neurons showed  
650 reduced activity when S1 was inactivated (Zhang et al., 1996), while 35% of S1 neurons  
651 showed reduced activity when S2 was inactivated (Zhang et al., 2001). This asymmetry could  
652 be due to anatomical asymmetries (for review see (Burton, 1986; Jones, 1986)), which led to  
653 the hypothesis that the S1 to S2 input represents a feed-forward projection, whereas the S2 to  
654 S1 input is a feed-back projection (Jones, 1986).

655

656 Together, while contralateral [ipsilesional] sensorimotor  $\beta$  rebound is reduced in low function  
657 patients and in patients who didn't recover, differences in functional and structural intra-  
658 hemispheric connectivity are unique to the level of motor function. Thus, one could argue that  
659 sensorimotor  $\beta$  rebound and good manual dexterity demand sufficient structural and functional  
660 integrity between the key sensorimotor areas.

661

### 662 **4.3 Inter-hemispheric connectivity differs as a function of** 663 **subsequent motor recovery**

664 Following intra-hemispheric connections, we next sought to evaluate the relevance of inter-  
665 hemispheric connections for post-stroke initial motor function and subsequent motor recovery.  
666 At the level of brain function, we observed recovery-related, but not function-related  
667 differences in inter-hemispheric disconnectivity. Specifically, we found that commissural  
668 motor connections were more disconnected in patients who didn't recover, compared to  
669 patients who recovered, which is in line with a previous study (Yu et al., 2019). The importance  
670 of commissural connections for post-stroke motor recovery is corroborated by studies  
671 investigating the microarchitecture of the corpus callosum in the chronic phase post-stroke.  
672 These studies found that injury to the corpus callosum caused by stroke lesions through axonal  
673 degeneration correlated with poor subsequent motor recovery (J. Chen & Schlaug, 2013; Li et  
674 al., 2015; Radlinska et al., 2012; Stewart et al., 2017; Wang et al., 2012).

675  
676 At the level of brain function, we found that inter-hemispheric connectivity was directed from  
677 the contralateral [ipsilesional] to the ipsilateral [contralesional] hemisphere in patients who  
678 recovered, while patients who didn't recover showed the opposite pattern. The pattern observed  
679 in patients who didn't recover, i.e., ipsilateral [contralesional] activity driving contralateral  
680 [ipsilesional] activity, can be interpreted in the light of the inter-hemispheric imbalance, related  
681 to decreased contralateral [ipsilesional] excitability and increased ipsilateral [contralesional]  
682 excitability (Nowak et al., 2009). As previous studies have focused almost exclusively on inter-  
683 hemispheric connectivity in M1 (Murase et al., 2004), the connectivity between the sensory  
684 areas is largely understudied ((Calautti et al., 2007), but see (Frías et al., 2018)). Combining  
685 tactile stimulation with high-quality MEG data, allowed us to investigate S1 and S2 in addition  
686 to M1. Our results suggest that the inter-hemispheric imbalance is not unique to M1 but extends  
687 to sensory areas. The inter-hemispheric imbalance framework informs non-invasive brain  
688 stimulation aiming at increasing contralateral [ipsilesional] excitability and decreasing  
689 ipsilateral [contralesional] excitability to enhance motor recovery post-stroke (Du et al., 2019;  
690 Lefebvre et al., 2013; Lindenberg et al., 2010; O'Shea et al., 2014; Ward & Cohen, 2004).

691  
692 In summary, we found that differences in inter-hemispheric structural and functional  
693 connectivity relate to recovery-related rather than function-related processes. We found that  
694 patients who recovered had more intact commissural motor connections and functional

695 connectivity directed from the contralateral [ipsilesional] to the ipsilateral [contralesional]  
696 hemisphere in acute brain imaging.

697

#### 698 **4.4 Predicting subsequent motor recovery post-stroke**

699 Capitalising on the group differences between patients who recovered and patients who didn't  
700 recover, we asked whether we could predict which of the low function patients will go on to  
701 achieve some recovery, based on very early post-stroke data. Generally, subsequent motor  
702 recovery is highly correlated to the initial function/impairment, however, this is not true for  
703 patients with initially severe upper limb impairment (Prabhakaran et al., 2008; Winters et al.,  
704 2015). Of these patients approximately half experience recovery while the other half do not  
705 (Winters et al., 2015). Therefore, there is a real need to improve outcome prediction in low  
706 function/more impaired patients. Here, we used properties from brain function and structure  
707 early post-stroke to predict whether low function patients were likely to recover or not. Model  
708 selection measures suggest a better model fit for the winning model, combining functional and  
709 structural features, compared to unimodal models. We found that, independent of initial  
710 severity, patients who had stronger functional inter-hemispheric connectivity and more intact  
711 motor projection connections were more likely to show subsequent motor recovery. Note that  
712 this prediction analysis focussed only on the subsample of initially low function patients. While  
713 this decision is mechanistically informed, it impacts the sample size. Further research focussing  
714 on the subsample of low function/more impaired patients are needed to fully uncover the  
715 mechanisms of recovery in this subsample.

716

#### 717 **4.5 Limitations and future directions**

718 Post-stroke initial motor function/impairment and subsequent motor recovery, as well as the  
719 accompanying changes in brain function and structure, are multifarious and highly complex.  
720 While we focus on an important subset of brain functional and brain structural features, it is  
721 nevertheless a subset of an enormous feature space. Dimensionality reduction through feature  
722 selection is a common approach in outcome prediction models but usually relies on a priori  
723 decision making. Unsupervised high-dimensional methods (such as (Schrouff et al., 2013)) can  
724 overcome this problem but need extremely large datasets. As structural brain data are acquired  
725 as part of the clinical routine in some countries, large datasets of structural data post-stroke  
726 exist (such as (Liew et al., 2020)). However, functional brain data is not acquired routinely,

727 and so there are no large datasets of functional brain data post stroke and large datasets  
728 combining brain structure and function.

729

730 As common practice, we collapsed right and left hemispheric strokes, however, the possibility  
731 of systematic differences in functional connectivity between left and right hemispheric strokes  
732 has been highlighted recently (Song et al., 2023). Collapsing across lesion side, as well as  
733 gender is, given the sample size, a pragmatic decision.

734

735 The functional and structural data used here were not acquired as part of clinical routines.  
736 However, to validate the results on large datasets and embed prediction models based on  
737 neuroimaging in clinical practice and care pathways the functional and structural features need  
738 to be extracted from inexpensive and accessible technology. To this end, high-quality MRI and  
739 MEG need to be replaced by routine scans and EEG. Strong correlation between MEG and  
740 EEG (Illman et al., 2020), as well as recent developments in mobile EEG (Niso et al., 2023)  
741 pave the way for low-cost assessment of functional measures at the bedside. Bedside recordings  
742 further allow the inclusion of underserved populations, i.e., patients with severe disabilities.  
743 Finally, to further improve prediction additional features, such as sensory impairment, other  
744 measurement depicting the quality of upper limb movement (Kwakkel et al., 2019), presence  
745 and strength of transcranial magnetic stimulation induced elicit motor-evoked potentials  
746 (Stinear et al., 2012), treatment type (i.e., thrombolysis or thrombectomy) stroke type (Grima  
747 et al., 2024), and several time points (acute and sub-acute stage) should be considered in future.

## 748 **Acknowledgments**

749 We thank Suvi Heikkilä, Jari Kainulainen, Jyrki Mäkelä and Mia Illman for their help with  
750 MEG data acquisition. The authors thank the HUS occupational therapist for performing  
751 clinical testing.

752

## 753 **Funding**

754 The study was financially supported by the Academy of Finland (National Centers of  
755 Excellence Program 2006–2011), the Helsinki University Central Hospital Research Fund, The  
756 Finnish Medical Foundation and Tekes, Finnish Funding Agency for Technology and  
757 Innovation, SalWe Research Program for Mind and Body and Seamless Patient Care Grant  
758 nos. 1104/10 and 1988/31/2015. CZ was supported by Brain Research UK (201718-13).

759

## 760 **Author contributions**

761 CZ: Conceptualization, Formal analysis, Methodology, Visualisation, Writing – original draft

762 NSW: Conceptualization, Funding acquisition, Writing – review and editing

763 NF: Conceptualization, Funding acquisition, Writing – review and editing

764 SV: Conceptualization, Writing – review and editing

765 AJQ: Methodology, Software, Writing – review and editing

766 EK: Data Curation, Project administration, Writing – original draft

767 KL: Conceptualization, Data Curation, Project administration, Writing – original draft

768

## 769 **Competing interests**

770 The authors report no competing interests.

771

## 772 **References**

773 Ageranioti-Bélanger, S. A., & Chapman, C. E. (1992). Discharge properties of neurones in the hand  
774 area of primary somatosensory cortex in monkeys in relation to the performance of an active  
775 tactile discrimination task. *Experimental Brain Research*, *91*(2), 207–228.

776 <https://doi.org/10.1007/BF00231655>

- 777 Alayrangues, J., Torrecillos, F., Jahani, A., & Malfait, N. (2019). Error-related modulations of the  
778 sensorimotor post-movement and foreperiod beta-band activities arise from distinct neural  
779 substrates and do not reflect efferent signal processing. *NeuroImage*, *184*, 10–24.  
780 <https://doi.org/10.1016/j.neuroimage.2018.09.013>
- 781 Alexander, L. D., Black, S. E., Gao, F., Szilagyi, G., Danells, C. J., & McIlroy, W. E. (2010).  
782 Correlating lesion size and location to deficits after ischemic stroke: The influence of  
783 accounting for altered peri-necrotic tissue and incidental silent infarcts. *Behavioral and Brain*  
784 *Functions*, *6*(1), 6. <https://doi.org/10.1186/1744-9081-6-6>
- 785 Baccalá, L. A., & Sameshima, K. (2001). Partial directed coherence: A new concept in neural  
786 structure determination. *Biological Cybernetics*, *84*(6), 463–474.  
787 <https://doi.org/10.1007/PL00007990>
- 788 Bardouille, T., Picton, T. W., & Ross, B. (2010). Attention modulates beta oscillations during  
789 prolonged tactile stimulation. *The European Journal of Neuroscience*, *31*(4), 761–769.  
790 <https://doi.org/10.1111/j.1460-9568.2010.07094.x>
- 791 Bastos, A. M., & Schoffelen, J.-M. (2016). A Tutorial Review of Functional Connectivity Analysis  
792 Methods and Their Interpretational Pitfalls. *Frontiers in Systems Neuroscience*, *9*.  
793 <https://doi.org/10.3389/fnsys.2015.00175>
- 794 Blinowska, K. J. (2011). Review of the methods of determination of directed connectivity from  
795 multichannel data. *Medical & Biological Engineering & Computing*, *49*(5), 521–529.  
796 <https://doi.org/10.1007/s11517-011-0739-x>
- 797 Brodie, S., Meehan, S., Borich, M., & Boyd, L. (2014). 5 Hz repetitive transcranial magnetic  
798 stimulation over the ipsilesional sensory cortex enhances motor learning after stroke.  
799 *Frontiers in Human Neuroscience*, *8*.  
800 <https://www.frontiersin.org/articles/10.3389/fnhum.2014.00143>
- 801 Broeks, J., LANKHORST, G. J., RUMPING, K., & PREVO, A. J. H. (1999). The long-term outcome  
802 of arm function after stroke: Results of a follow-up study. *Disability and Rehabilitation*,  
803 *21*(8), 357–364. <https://doi.org/10.1080/096382899297459>

- 804 Burton, H. (1986). Second Somatosensory Cortex and Related Areas. In E. G. Jones & A. Peters  
805 (Eds.), *Sensory-Motor Areas and Aspects of Cortical Connectivity* (pp. 31–98). Springer US.  
806 [https://doi.org/10.1007/978-1-4613-2149-1\\_2](https://doi.org/10.1007/978-1-4613-2149-1_2)
- 807 Byblow, W. D., Stinear, C. M., Barber, P. A., Petoe, M. A., & Ackerley, S. J. (2015). Proportional  
808 recovery after stroke depends on corticomotor integrity. *Annals of Neurology*, 78(6), 848–  
809 859. <https://doi.org/10.1002/ana.24472>
- 810 Calautti, C., Naccarato, M., Jones, P. S., Sharma, N., Day, D. D., Carpenter, A. T., Bullmore, E. T.,  
811 Warburton, E. A., & Baron, J.-C. (2007). The relationship between motor deficit and  
812 hemisphere activation balance after stroke: A 3T fMRI study. *NeuroImage*, 34(1), 322–331.  
813 <https://doi.org/10.1016/j.neuroimage.2006.08.026>
- 814 Campos, B., Choi, H., DeMarco, A. T., Seydell-Greenwald, A., Hussain, S. J., Joy, M. T., Turkeltaub,  
815 P. E., & Zeiger, W. (2023). Rethinking Remapping: Circuit Mechanisms of Recovery after  
816 Stroke. *The Journal of Neuroscience*, 43(45), 7489–7500.  
817 <https://doi.org/10.1523/JNEUROSCI.1425-23.2023>
- 818 Carmichael, S. T. (2012). Brain Excitability in Stroke: The Yin and Yang of Stroke Progression.  
819 *Archives of Neurology*, 69(2), 161–167. <https://doi.org/10.1001/archneurol.2011.1175>
- 820 Chen, C.-L., Tang, F.-T., Chen, H.-C., Chung, C.-Y., & Wong, M.-K. (2000). Brain lesion size and  
821 location: Effects on motor recovery and functional outcome in stroke patients. *Archives of*  
822 *Physical Medicine and Rehabilitation*, 81(4), 447–452. <https://doi.org/10.1053/mr.2000.3837>
- 823 Chen, J., & Schlaug, G. (2013). Resting State Interhemispheric Motor Connectivity and White Matter  
824 Integrity Correlate with Motor Impairment in Chronic Stroke. *Frontiers in Neurology*, 4.  
825 <https://www.frontiersin.org/articles/10.3389/fneur.2013.00178>
- 826 Chen, R., & Hallett, M. (1999). The time course of changes in motor cortex excitability associated  
827 with voluntary movement. *The Canadian Journal of Neurological Sciences. Le Journal*  
828 *Canadien Des Sciences Neurologiques*, 26(3), 163–169.  
829 <https://doi.org/10.1017/s0317167100000196>

- 830 Clarkson, A. N., Huang, B. S., MacIsaac, S. E., Mody, I., & Carmichael, S. T. (2010). Reducing  
831 excessive GABA-mediated tonic inhibition promotes functional recovery after stroke. *Nature*,  
832 *468*(7321), Article 7321. <https://doi.org/10.1038/nature09511>
- 833 Colclough, G. L., Brookes, M. J., Smith, S. M., & Woolrich, M. W. (2015). A symmetric multivariate  
834 leakage correction for MEG connectomes. *NeuroImage*, *117*, 439–448.  
835 <https://doi.org/10.1016/j.neuroimage.2015.03.071>
- 836 Colclough, G. L., Woolrich, M. W., Tewarie, P. K., Brookes, M. J., Quinn, A. J., & Smith, S. M.  
837 (2016). How reliable are MEG resting-state connectivity metrics? *NeuroImage*, *138*, 284–  
838 293. <https://doi.org/10.1016/j.neuroimage.2016.05.070>
- 839 de Freitas Zanona, A., Romeiro da Silva, A. C., Baltar do Rego Maciel, A., Shirahige Gomes do  
840 Nascimento, L., Bezerra da Silva, A., Piscitelli, D., & Monte-Silva, K. (2023). Sensory and  
841 motor cortical excitability changes induced by rTMS and sensory stimulation in stroke: A  
842 randomized clinical trial. *Frontiers in Neuroscience*, *16*.  
843 <https://www.frontiersin.org/articles/10.3389/fnins.2022.985754>
- 844 de Haan, B., Clas, P., Juenger, H., Wilke, M., & Karnath, H.-O. (2015). Fast semi-automated lesion  
845 demarcation in stroke. *NeuroImage: Clinical*, *9*, 69–74.  
846 <https://doi.org/10.1016/j.nicl.2015.06.013>
- 847 Disbrow, E., Litinas, E., Recanzone, G. H., Padberg, J., & Krubitzer, L. (2003). Cortical connections  
848 of the second somatosensory area and the parietal ventral area in macaque monkeys. *Journal*  
849 *of Comparative Neurology*, *462*(4), 382–399. <https://doi.org/10.1002/cne.10731>
- 850 Disbrow, E., Litinas, E., Recanzone, G., Slutsky, D., & Krubitzer, L. (2002). Thalamocortical  
851 connections of the parietal ventral area (PV) and the second somatosensory area (S2) in  
852 macaque monkeys. *Thalamus & Related Systems*, *1*(4), 289–302.  
853 <https://doi.org/10.1017/S1472928802000031>
- 854 Disbrow, E., Roberts, T., Poeppel, D., & Krubitzer, L. (2001). Evidence for Interhemispheric  
855 Processing of Inputs From the Hands in Human S2 and PV. *Journal of Neurophysiology*,  
856 *85*(5), 2236–2244. <https://doi.org/10.1152/jn.2001.85.5.2236>



- 857 Du, J., Yang, F., Hu, J., Hu, J., Xu, Q., Cong, N., Zhang, Q., Liu, L., Mantini, D., Zhang, Z., Lu, G.,  
858 & Liu, X. (2019). Effects of high- and low-frequency repetitive transcranial magnetic  
859 stimulation on motor recovery in early stroke patients: Evidence from a randomized  
860 controlled trial with clinical, neurophysiological and functional imaging assessments.  
861 *NeuroImage. Clinical*, 21, 101620. <https://doi.org/10.1016/j.nicl.2018.101620>
- 862 Egger, P., Evangelista, G. G., Koch, P. J., Park, C.-H., Levin-Gleba, L., Girard, G., Beanato, E., Lee,  
863 J., Choirat, C., Guggisberg, A. G., Kim, Y.-H., & Hummel, F. C. (2021). Disconnectomics of  
864 the Rich Club Impacts Motor Recovery After Stroke. *Stroke*, 52(6), 2115–2124.  
865 <https://doi.org/10.1161/STROKEAHA.120.031541>
- 866 Espenhahn, S., de Berker, A. O., van Wijk, B. C. M., Rossiter, H. E., & Ward, N. S. (2017).  
867 Movement-related beta oscillations show high intra-individual reliability. *NeuroImage*, 147,  
868 175–185. <https://doi.org/10.1016/j.neuroimage.2016.12.025>
- 869 Espenhahn, S., Rossiter, H. E., van Wijk, B. C. M., Redman, N., Rondina, J. M., Diedrichsen, J., &  
870 Ward, N. S. (2020). Sensorimotor cortex beta oscillations reflect motor skill learning ability  
871 after stroke. *Brain Communications*, 2(2), fcaa161.  
872 <https://doi.org/10.1093/braincomms/fcaa161>
- 873 Franzkowiak, S., Pollok, B., Biermann-Ruben, K., Südmeyer, M., Paszek, J., Jonas, M., Thomalla, G.,  
874 Bäumer, T., Orth, M., Münchau, A., & Schnitzler, A. (2010). Altered pattern of motor cortical  
875 activation-inhibition during voluntary movements in Tourette syndrome. *Movement*  
876 *Disorders: Official Journal of the Movement Disorder Society*, 25(12), 1960–1966.  
877 <https://doi.org/10.1002/mds.23186>
- 878 Frías, I., Starrs, F., Gisiger, T., Minuk, J., Thiel, A., & Paquette, C. (2018). Interhemispheric  
879 connectivity of primary sensory cortex is associated with motor impairment after stroke.  
880 *Scientific Reports*, 8(1), Article 1. <https://doi.org/10.1038/s41598-018-29751-6>
- 881 Friedman, D. P., & Murray, E. A. (1986). Thalamic connectivity of the second somatosensory area  
882 and neighboring somatosensory fields of the lateral sulcus of the macaque. *Journal of*  
883 *Comparative Neurology*, 252(3), 348–373. <https://doi.org/10.1002/cne.902520305>

- 884 Gaetz, W., & Cheyne, D. (2006). Localization of sensorimotor cortical rhythms induced by tactile  
885 stimulation using spatially filtered MEG. *NeuroImage*, *30*(3), 899–908.  
886 <https://doi.org/10.1016/j.neuroimage.2005.10.009>
- 887 Gaetz, W., Edgar, J. C., & Roberts, D. J. W. T. P. L. (2011). Relating MEG Measured Motor Cortical  
888 Oscillations to resting  $\gamma$ -Aminobutyric acid (GABA) Concentration. *NeuroImage*, *55*(2), 616–  
889 621. <https://doi.org/10.1016/j.neuroimage.2010.12.077>
- 890 Gandolla, M., Niero, L., Molteni, F., Guanzioli, E., Ward, N. S., & Pedrocchi, A. (2021). Brain  
891 Plasticity Mechanisms Underlying Motor Control Reorganization: Pilot Longitudinal Study  
892 on Post-Stroke Subjects. *Brain Sciences*, *11*(3), 329.  
893 <https://doi.org/10.3390/brainsci11030329>
- 894 Garry, M. I., Loftus, A., & Summers, J. J. (2005). Mirror, mirror on the wall: Viewing a mirror  
895 reflection of unilateral hand movements facilitates ipsilateral M1 excitability. *Experimental*  
896 *Brain Research*, *163*(1), 118–122. <https://doi.org/10.1007/s00221-005-2226-9>
- 897 Griffis, J. C., Metcalf, N. V., Corbetta, M., & Shulman, G. L. (2019). Structural Disconnections  
898 Explain Brain Network Dysfunction after Stroke. *Cell Reports*, *28*(10), 2527-2540.e9.  
899 <https://doi.org/10.1016/j.celrep.2019.07.100>
- 900 Griffis, J. C., Metcalf, N. V., Corbetta, M., & Shulman, G. L. (2021). Lesion Quantification Toolkit:  
901 A MATLAB software tool for estimating grey matter damage and white matter  
902 disconnections in patients with focal brain lesions. *NeuroImage: Clinical*, *30*, 102639.  
903 <https://doi.org/10.1016/j.nicl.2021.102639>
- 904 Grima, L., Davenport, S., Parry-Jones, A. R., Vail, A., & Hammerbeck, U. (2024). *Comparing motor*  
905 *recovery in ischaemic stroke ... | Health Open Research*.  
906 <https://healthopenresearch.org/articles/5-33>
- 907 Haar, S., & Faisal, A. A. (2020). Brain Activity Reveals Multiple Motor-Learning Mechanisms in a  
908 Real-World Task. *Frontiers in Human Neuroscience*, *14*, 354.  
909 <https://doi.org/10.3389/fnhum.2020.00354>
- 910 Hall, S. D., Barnes, G. R., Furlong, P. L., Seri, S., & Hillebrand, A. (2010). Neuronal network  
911 pharmacodynamics of GABAergic modulation in the human cortex determined using

- 912           pharmaco-magnetoencephalography. *Human Brain Mapping*, 31(4), 581–594.  
913           <https://doi.org/10.1002/hbm.20889>
- 914   Hamdy, S., Rothwell, J. C., Aziz, Q., Singh, K. D., & Thompson, D. G. (1998). Long-term  
915           reorganization of human motor cortex driven by short-term sensory stimulation. *Nature*  
916           *Neuroscience*, 1(1), 64–68. <https://doi.org/10.1038/264>
- 917   Hari, R., Forss, N., Avikainen, S., Kirveskari, E., Salenius, S., & Rizzolatti, G. (1998). Activation of  
918           human primary motor cortex during action observation: A neuromagnetic study. *Proceedings*  
919           *of the National Academy of Sciences*, 95(25), 15061–15065.  
920           <https://doi.org/10.1073/pnas.95.25.15061>
- 921   Harris, C. R., Millman, K. J., van der Walt, S. J., Gommers, R., Virtanen, P., Cournapeau, D., Wieser,  
922           E., Taylor, J., Berg, S., Smith, N. J., Kern, R., Picus, M., Hoyer, S., van Kerkwijk, M. H.,  
923           Brett, M., Haldane, A., del Río, J. F., Wiebe, M., Peterson, P., ... Oliphant, T. E. (2020).  
924           Array programming with NumPy. *Nature*, 585(7825), Article 7825.  
925           <https://doi.org/10.1038/s41586-020-2649-2>
- 926   Hinkley, L. B., Krubitzer, L. A., Nagarajan, S. S., & Disbrow, E. A. (2007). Sensorimotor Integration  
927           in S2, PV, and Parietal Rostroventral Areas of the Human Sylvian Fissure. *Journal of*  
928           *Neurophysiology*, 97(2), 1288–1297. <https://doi.org/10.1152/jn.00733.2006>
- 929   Hyvarinen, A. (1999). Fast and robust fixed-point algorithms for independent component analysis.  
930           *IEEE Transactions on Neural Networks*, 10(3), 626–634. <https://doi.org/10.1109/72.761722>
- 931   Illman, M., Laaksonen, K., Liljeström, M., Jousmäki, V., Piitulainen, H., & Forss, N. (2020).  
932           Comparing MEG and EEG in detecting the ~20-Hz rhythm modulation to tactile and  
933           proprioceptive stimulation. *NeuroImage*, 215, 116804.  
934           <https://doi.org/10.1016/j.neuroimage.2020.116804>
- 935   Illman, M., Laaksonen, K., Liljeström, M., Piitulainen, H., & Forss, N. (2021). The effect of alertness  
936           and attention on the modulation of the beta rhythm to tactile stimulation. *Physiological*  
937           *Reports*, 9(12), e14818. <https://doi.org/10.14814/phy2.14818>

- 938 Inoue, K., Yamashita, T., Harada, T., & Nakamura, S. (2002). Role of human SII cortices in  
939 sensorimotor integration. *Clinical Neurophysiology*, *113*(10), 1573–1578.  
940 [https://doi.org/10.1016/S1388-2457\(02\)00162-1](https://doi.org/10.1016/S1388-2457(02)00162-1)
- 941 Ito, K. L., Kim, H., & Liew, S. (2019). A comparison of automated lesion segmentation approaches  
942 for chronic stroke T1-weighted MRI data. *Human Brain Mapping*, *40*(16), 4669–4685.  
943 <https://doi.org/10.1002/hbm.24729>
- 944 Jensen, O., Goel, P., Kopell, N., Pohja, M., Hari, R., & Ermentrout, B. (2005). On the human  
945 sensorimotor-cortex beta rhythm: Sources and modeling. *NeuroImage*, *26*(2), 347–355.  
946 <https://doi.org/10.1016/j.neuroimage.2005.02.008>
- 947 Jones, E. G. (Ed.). (1985). *The Thalamus*. Springer US. <https://doi.org/10.1007/978-1-4615-1749-8>
- 948 Jones, E. G. (1986). Connectivity of the Primate Sensory-Motor Cortex. In E. G. Jones & A. Peters  
949 (Eds.), *Sensory-Motor Areas and Aspects of Cortical Connectivity* (pp. 113–183). Springer  
950 US. [https://doi.org/10.1007/978-1-4613-2149-1\\_4](https://doi.org/10.1007/978-1-4613-2149-1_4)
- 951 Kinnischtzke, A. K., Fanselow, E. E., & Simons, D. J. (2016). Target-specific M1 inputs to  
952 infragranular S1 pyramidal neurons. *Journal of Neurophysiology*, *116*(3), 1261–1274.  
953 <https://doi.org/10.1152/jn.01032.2015>
- 954 Krubitzer, L. A., & Kaas, J. H. (1990). The organization and connections of somatosensory cortex in  
955 marmosets. *Journal of Neuroscience*, *10*(3), 952–974.  
956 <https://doi.org/10.1523/JNEUROSCI.10-03-00952.1990>
- 957 Kwakkel, G., van Wegen, E. E. H., Burridge, J. H., Winstein, C. J., van Dokkum, L. E. H., Alt  
958 Murphy, M., Levin, M. F., Krakauer, J. W., Lang, C. E., Keller, T., Kitago, T., Nordin, N.,  
959 Pomeroy, V., Veerbeek, J. M., & van Wijck, F. (2019). Standardized Measurement of Quality  
960 of Upper Limb Movement After Stroke: Consensus-Based Core Recommendations From the  
961 Second Stroke Recovery and Rehabilitation Roundtable. *Neurorehabilitation and Neural  
962 Repair*, *33*(11), 951–958. <https://doi.org/10.1177/1545968319886477>
- 963 Laaksonen, K., Kirveskari, E., Mäkelä, J. P., Kaste, M., Mustanoja, S., Nummenmaa, L., Tatlisumak,  
964 T., & Forss, N. (2012). Effect of afferent input on motor cortex excitability during stroke

- 965 recovery. *Clinical Neurophysiology*, 123(12), 2429–2436.
- 966 <https://doi.org/10.1016/j.clinph.2012.05.017>
- 967 Lefebvre, S., Laloux, P., Peeters, A., Desfontaines, P., Jamart, J., & Vandermeeren, Y. (2013). Dual-  
968 tDCS Enhances Online Motor Skill Learning and Long-Term Retention in Chronic Stroke  
969 Patients. *Frontiers in Human Neuroscience*, 6.  
970 <https://www.frontiersin.org/articles/10.3389/fnhum.2012.00343>
- 971 Levin, M. F., Kleim, J. A., & Wolf, S. L. (2009). What do motor ‘recovery’ and ‘compensation’ mean  
972 in patients following stroke? *Neurorehabilitation and Neural Repair*, 23(4), 313–319.  
973 <https://doi.org/10.1177/1545968308328727>
- 974 Lewis, J. W., & Van Essen, D. C. (2000). Corticocortical connections of visual, sensorimotor, and  
975 multimodal processing areas in the parietal lobe of the macaque monkey. *Journal of*  
976 *Comparative Neurology*, 428(1), 112–137. [https://doi.org/10.1002/1096-](https://doi.org/10.1002/1096-9861(20001204)428:1<112::AID-CNE8>3.0.CO;2-9)  
977 [9861\(20001204\)428:1<112::AID-CNE8>3.0.CO;2-9](https://doi.org/10.1002/1096-9861(20001204)428:1<112::AID-CNE8>3.0.CO;2-9)
- 978 Li, Y., Wu, P., Liang, F., & Huang, W. (2015). The Microstructural Status of the Corpus Callosum Is  
979 Associated with the Degree of Motor Function and Neurological Deficit in Stroke Patients.  
980 *PLOS ONE*, 10(4), e0122615. <https://doi.org/10.1371/journal.pone.0122615>
- 981 Liew, S., Zavaliangos-Petropulu, A., Jahanshad, N., Lang, C. E., Hayward, K. S., Lohse, K. R.,  
982 Juliano, J. M., Assogna, F., Baugh, L. A., Bhattacharya, A. K., Bigjahan, B., Borich, M. R.,  
983 Boyd, L. A., Brodtmann, A., Buetefisch, C. M., Byblow, W. D., Cassidy, J. M., Conforto, A.  
984 B., Craddock, R. C., ... Thompson, P. M. (2020). The ENIGMA Stroke Recovery Working  
985 Group: Big data neuroimaging to study brain–behavior relationships after stroke. *Human*  
986 *Brain Mapping*, 43(1), 129–148. <https://doi.org/10.1002/hbm.25015>
- 987 Lindenberg, R., Renga, V., Zhu, L. L., Nair, D., & Schlaug, G. (2010). Bihemispheric brain  
988 stimulation facilitates motor recovery in chronic stroke patients. *Neurology*, 75(24), 2176–  
989 2184. <https://doi.org/10.1212/WNL.0b013e318202013a>
- 990 Mäkelä, J. P., Lioumis, P., Laaksonen, K., Forss, N., Tatlisumak, T., Kaste, M., & Mustanoja, S.  
991 (2015). Cortical Excitability Measured with nTMS and MEG during Stroke Recovery. *Neural*  
992 *Plasticity*, 2015, 309546. <https://doi.org/10.1155/2015/309546>

- 993 Maraka, S., Jiang, Q., Jafari-Khouzani, K., Li, L., Malik, S., Hamidian, H., Zhang, T., Lu, M.,  
994 Soltanian-Zadeh, H., Chopp, M., & Mitsias, P. D. (2014). Degree of corticospinal tract  
995 damage correlates with motor function after stroke. *Annals of Clinical and Translational*  
996 *Neurology*, *1*(11), 891–899. <https://doi.org/10.1002/acn3.132>
- 997 Maris, E., & Oostenveld, R. (2007). Nonparametric statistical testing of EEG- and MEG-data. *Journal*  
998 *of Neuroscience Methods*, *164*(1), 177–190. <https://doi.org/10.1016/j.jneumeth.2007.03.024>
- 999 Motolese, F., Lanzone, J., Todisco, A., Rossi, M., Santoro, F., Cruciani, A., Capone, F., Di Lazzaro,  
1000 V., & Pilato, F. (2023). The role of neurophysiological tools in the evaluation of ischemic  
1001 stroke evolution: A narrative review. *Frontiers in Neurology*, *14*.  
1002 <https://doi.org/10.3389/fneur.2023.1178408>
- 1003 Mountcastle, V. B. (1978). An organizing principle for cerebral function: The unit module and the  
1004 distributed system. In *The Mindful Brain* (pp. 7–50). MIT.
- 1005 Mountcastle, V. B. (1986). The neural mechanisms of cognitive functions can now be studied directly.  
1006 *Trends in Neurosciences*, *9*, 505–508. [https://doi.org/10.1016/0166-2236\(86\)90160-8](https://doi.org/10.1016/0166-2236(86)90160-8)
- 1007 Murase, N., Duque, J., Mazzocchio, R., & Cohen, L. G. (2004). Influence of interhemispheric  
1008 interactions on motor function in chronic stroke. *Annals of Neurology*, *55*(3), 400–409.  
1009 <https://doi.org/10.1002/ana.10848>
- 1010 Nichols, T. E., & Holmes, A. P. (2002). Nonparametric permutation tests for functional  
1011 neuroimaging: A primer with examples. *Human Brain Mapping*, *15*(1), 1–25.  
1012 <https://doi.org/10.1002/hbm.1058>
- 1013 Niso, G., Romero, E., Moreau, J. T., Araujo, A., & Krol, L. R. (2023). Wireless EEG: A survey of  
1014 systems and studies. *NeuroImage*, *269*, 119774.  
1015 <https://doi.org/10.1016/j.neuroimage.2022.119774>
- 1016 Nowak, D. A., Grefkes, C., Ameli, M., & Fink, G. R. (2009). Interhemispheric competition after  
1017 stroke: Brain stimulation to enhance recovery of function of the affected hand.  
1018 *Neurorehabilitation and Neural Repair*, *23*(7), 641–656.  
1019 <https://doi.org/10.1177/1545968309336661>

- 1020 O'Shea, J., Boudrias, M.-H., Stagg, C. J., Bachtiar, V., Kischka, U., Blicher, J. U., & Johansen-Berg,  
1021 H. (2014). Predicting behavioural response to TDCS in chronic motor stroke. *NeuroImage*, 85  
1022 Pt 3(Pt 3), 924–933. <https://doi.org/10.1016/j.neuroimage.2013.05.096>
- 1023 Parkkonen, E., Laaksonen, K., Parkkonen, L., & Forss, N. (2018). Recovery of the 20 Hz Rebound to  
1024 Tactile and Proprioceptive Stimulation after Stroke. *Neural Plasticity*, 2018, 1–11.  
1025 <https://doi.org/10.1155/2018/7395798>
- 1026 Parkkonen, E., Laaksonen, K., Piitulainen, H., Pekkola, J., Parkkonen, L., Tatlisumak, T., & Forss, N.  
1027 (2017). Strength of ~20-Hz Rebound and Motor Recovery After Stroke. *Neurorehabilitation*  
1028 *and Neural Repair*, 31(5), 475–486. <https://doi.org/10.1177/1545968316688795>
- 1029 Petrof, I., Viaene, A. N., & Sherman, S. M. (2015). Properties of the primary somatosensory cortex  
1030 projection to the primary motor cortex in the mouse. *Journal of Neurophysiology*, 113(7),  
1031 2400–2407. <https://doi.org/10.1152/jn.00949.2014>
- 1032 Pfurtscheller, G. (1992). Event-related synchronization (ERS): An electrophysiological correlate of  
1033 cortical areas at rest. *Electroencephalography and Clinical Neurophysiology*, 83(1), 62–69.  
1034 [https://doi.org/10.1016/0013-4694\(92\)90133-3](https://doi.org/10.1016/0013-4694(92)90133-3)
- 1035 Prabhakaran, S., Zarahn, E., Riley, C., Speizer, A., Chong, J. Y., Lazar, R. M., Marshall, R. S., &  
1036 Krakauer, J. W. (2008). Inter-individual Variability in the Capacity for Motor Recovery After  
1037 Ischemic Stroke. *Neurorehabilitation and Neural Repair*, 22(1), 64–71.  
1038 <https://doi.org/10.1177/1545968307305302>
- 1039 Puig, J., Blasco, G., Schlaug, G., Stinear, C. M., Daunis-i-Estadella, P., Biarnes, C., Figueras, J.,  
1040 Serena, J., Hernández-Pérez, M., Alberich-Bayarri, A., Castellanos, M., Liebeskind, D. S.,  
1041 Demchuk, A. M., Menon, B. K., Thomalla, G., Nael, K., Wintermark, M., & Pedraza, S.  
1042 (2017). Diffusion tensor imaging as a prognostic biomarker for motor recovery and  
1043 rehabilitation after stroke. *Neuroradiology*, 59(4), 343–351. [https://doi.org/10.1007/s00234-](https://doi.org/10.1007/s00234-017-1816-0)  
1044 [017-1816-0](https://doi.org/10.1007/s00234-017-1816-0)
- 1045 Quinn, A. J., Green, G. G. R., & Hymers, M. (2021). Delineating between-subject heterogeneity in  
1046 alpha networks with Spatio-Spectral Eigenmodes. *NeuroImage*, 240, 118330.  
1047 <https://doi.org/10.1016/j.neuroimage.2021.118330>

- 1048 Quinn, A. J., & Hymers, M. (2020). SAILS: Spectral Analysis In Linear Systems. *Journal of Open*  
1049 *Source Software*, 5(47), 1982. <https://doi.org/10.21105/joss.01982>
- 1050 Radlinska, B. A., Blunk, Y., Leppert, I. R., Minuk, J., Pike, G. B., & Thiel, A. (2012). Changes in  
1051 Callosal Motor Fiber Integrity after Subcortical Stroke of the Pyramidal Tract. *Journal of*  
1052 *Cerebral Blood Flow & Metabolism*, 32(8), 1515–1524.  
1053 <https://doi.org/10.1038/jcbfm.2012.37>
- 1054 Rapisarda, G., Bastings, E., de Noordhout, A. M., Pennisi, G., & Delwaide, P. j. (1996). Can Motor  
1055 Recovery in Stroke Patients Be Predicted by Early Transcranial Magnetic Stimulation?  
1056 *Stroke*, 27(12), 2191–2196. <https://doi.org/10.1161/01.STR.27.12.2191>
- 1057 Ridding, M. C., & Ziemann, U. (2010). Determinants of the induction of cortical plasticity by non-  
1058 invasive brain stimulation in healthy subjects. *The Journal of Physiology*, 588(13), 2291–  
1059 2304. <https://doi.org/10.1113/jphysiol.2010.190314>
- 1060 Roiha, K., Kirveskari, E., Kaste, M., Mustanoja, S., Mäkelä, J. P., Salonen, O., Tatlisumak, T., &  
1061 Forss, N. (2011). Reorganization of the primary somatosensory cortex during stroke recovery.  
1062 *Clinical Neurophysiology*, 122(2), 339–345. <https://doi.org/10.1016/j.clinph.2010.06.032>
- 1063 Rondina, J. M., Filippone, M., Girolami, M., & Ward, N. S. (2016). Decoding post-stroke motor  
1064 function from structural brain imaging. *NeuroImage: Clinical*, 12, 372–380.  
1065 <https://doi.org/10.1016/j.nicl.2016.07.014>
- 1066 Rondina, J. M., Park, C., & Ward, N. S. (2017). Brain regions important for recovery after severe  
1067 post-stroke upper limb paresis. *Journal of Neurology, Neurosurgery & Psychiatry*, 88(9),  
1068 737–743. <https://doi.org/10.1136/jnnp-2016-315030>
- 1069 Rosner, B. (1983). Percentage Points for a Generalized ESD Many-Outlier Procedure. *Technometrics*,  
1070 25(2), 9.
- 1071 Rothi, L. J., & Horner, J. (1983). Restitution and substitution: Two theories of recovery with  
1072 application to neurobehavioral treatment. *Journal of Clinical Neuropsychology*, 5(1), 73–81.  
1073 <https://doi.org/10.1080/01688638308401152>
- 1074 Rowe, M. J., Turman, A. B., Murray, G. M., & Zhang, H. Q. (1996). Parallel processing in  
1075 somatosensory areas I and II of the cerebral cortex. In O. Franzén, R. Johansson, & L.



- 1076 Terenius (Eds.), *Somesthesia and the Neurobiology of the Somatosensory Cortex* (pp. 197–  
1077 211). Birkhäuser. [https://doi.org/10.1007/978-3-0348-9016-8\\_18](https://doi.org/10.1007/978-3-0348-9016-8_18)
- 1078 Rudrauf, D., Mehta, S., & Grabowski, T. J. (2008). Disconnection’s renaissance takes shape: Formal  
1079 incorporation in group-level lesion studies. *Cortex; a Journal Devoted to the Study of the*  
1080 *Nervous System and Behavior*, 44(8), 1084–1096.  
1081 <https://doi.org/10.1016/j.cortex.2008.05.005>
- 1082 Salenius, S., Portin, K., Kajola, M., Salmelin, R., & Hari, R. (1997). Cortical Control of Human  
1083 Motoneuron Firing During Isometric Contraction. *Journal of Neurophysiology*, 77(6), 3401–  
1084 3405. <https://doi.org/10.1152/jn.1997.77.6.3401>
- 1085 Salmelin, R., Hämäläinen, M., Kajola, M., & Hari, R. (1995). Functional segregation of movement-  
1086 related rhythmic activity in the human brain. *NeuroImage*, 2(4), 237–243.  
1087 <https://doi.org/10.1006/nimg.1995.1031>
- 1088 Salmelin, R., & Hari, R. (1994). Spatiotemporal characteristics of sensorimotor neuromagnetic  
1089 rhythms related to thumb movement. *Neuroscience*, 60(2), 537–550.  
1090 [https://doi.org/10.1016/0306-4522\(94\)90263-1](https://doi.org/10.1016/0306-4522(94)90263-1)
- 1091 Schrouff, J., Rosa, M. J., Rondina, J. M., Marquand, A. F., Chu, C., Ashburner, J., Phillips, C.,  
1092 Richiardi, J., & Mourão-Miranda, J. (2013). PRoNTTo: Pattern Recognition for Neuroimaging  
1093 Toolbox. *Neuroinformatics*, 11(3), 319–337. <https://doi.org/10.1007/s12021-013-9178-1>
- 1094 Schulz, R., Park, C.-H., Boudrias, M.-H., Gerloff, C., Hummel, F. C., & Ward, N. S. (2012).  
1095 Assessing the integrity of corticospinal pathways from primary and secondary cortical motor  
1096 areas after stroke. *Stroke*, 43(8), 2248–2251.  
1097 <https://doi.org/10.1161/STROKEAHA.112.662619>
- 1098 Seghier, M. L. (2023). The elusive metric of lesion load. *Brain Structure and Function*.  
1099 <https://doi.org/10.1007/s00429-023-02630-1>
- 1100 Song, Y., Sun, Z., Sun, W., Luo, M., Du, Y., Jing, J., & Wang, Y. (2023). Neuroplasticity Following  
1101 Stroke from a Functional Laterality Perspective: A fNIRS Study. *Brain Topography*, 36(3),  
1102 283–293. <https://doi.org/10.1007/s10548-023-00946-z>

- 1103 Stewart, J. C., Dewanjee, P., Tran, G., Quinlan, E. B., Dodakian, L., McKenzie, A., See, J., & Cramer,  
1104 S. C. (2017). Role of corpus callosum integrity in arm function differs based on motor  
1105 severity after stroke. *NeuroImage: Clinical*, *14*, 641–647.  
1106 <https://doi.org/10.1016/j.nicl.2017.02.023>
- 1107 Stinear, C. M., Barber, P. A., Petoe, M., Anwar, S., & Byblow, W. D. (2012). The PREP algorithm  
1108 predicts potential for upper limb recovery after stroke. *Brain*, *135*(8), 2527–2535.  
1109 <https://doi.org/10.1093/brain/aws146>
- 1110 Stinear, C. M., Barber, P. A., Smale, P. R., Coxon, J. P., Fleming, M. K., & Byblow, W. D. (2007).  
1111 Functional potential in chronic stroke patients depends on corticospinal tract integrity. *Brain:*  
1112 *A Journal of Neurology*, *130*(Pt 1), 170–180. <https://doi.org/10.1093/brain/awl333>
- 1113 Swayne, O. B. C., Rothwell, J. C., Ward, N. S., & Greenwood, R. J. (2008). Stages of Motor Output  
1114 Reorganization after Hemispheric Stroke Suggested by Longitudinal Studies of Cortical  
1115 Physiology. *Cerebral Cortex*, *18*(8), 1909–1922. <https://doi.org/10.1093/cercor/bhm218>
- 1116 Talelli, P., Greenwood, R. J., & Rothwell, J. C. (2006). Arm function after stroke: Neurophysiological  
1117 correlates and recovery mechanisms assessed by transcranial magnetic stimulation. *Clinical*  
1118 *Neurophysiology*, *117*(8), 1641–1659. <https://doi.org/10.1016/j.clinph.2006.01.016>
- 1119 Talozzi, L., Forkel, S. J., Pacella, V., Nozais, V., Allart, E., Piscicelli, C., Pérennou, D., Tranel, D.,  
1120 Boes, A., Corbetta, M., Nachev, P., & Thiebaut De Schotten, M. (2023). Latent  
1121 disconnectome prediction of long-term cognitive-behavioural symptoms in stroke. *Brain*,  
1122 awad013. <https://doi.org/10.1093/brain/awad013>
- 1123 Tan, H., Jenkinson, N., & Brown, P. (2014). Dynamic Neural Correlates of Motor Error Monitoring  
1124 and Adaptation during Trial-to-Trial Learning. *Journal of Neuroscience*, *34*(16), 5678–5688.  
1125 <https://doi.org/10.1523/JNEUROSCI.4739-13.2014>
- 1126 Tan, H., Wade, C., & Brown, P. (2016). Post-Movement Beta Activity in Sensorimotor Cortex  
1127 Indexes Confidence in the Estimations from Internal Models. *Journal of Neuroscience*, *36*(5),  
1128 1516–1528. <https://doi.org/10.1523/JNEUROSCI.3204-15.2016>
- 1129 Tang, C.-W., Hsiao, F.-J., Lee, P.-L., Tsai, Y.-A., Hsu, Y.-F., Chen, W.-T., Lin, Y.-Y., Stagg, C. J., &  
1130 Lee, I.-H. (2020).  $\beta$ -Oscillations Reflect Recovery of the Paretic Upper Limb in Subacute

- 1131           Stroke. *Neurorehabilitation and Neural Repair*, 34(5), 450–462.
- 1132           <https://doi.org/10.1177/1545968320913502>
- 1133   Torrecillos, F., Tinkhauser, G., Fischer, P., Green, A. L., Aziz, T. Z., Foltynie, T., Limousin, P.,  
1134           Zrinzo, L., Ashkan, K., Brown, P., & Tan, H. (2018). Modulation of Beta Bursts in the  
1135           Subthalamic Nucleus Predicts Motor Performance. *The Journal of Neuroscience*, 38(41),  
1136           8905–8917. <https://doi.org/10.1523/JNEUROSCI.1314-18.2018>
- 1137   Van Veen, B. D., & Buckley, K. M. (1988). Beamforming: A versatile approach to spatial filtering.  
1138           *IEEE ASSP Magazine*, 5(2), 4–24. <https://doi.org/10.1109/53.665>
- 1139   Virtanen, P., Gommers, R., Oliphant, T. E., Haberland, M., Reddy, T., Cournapeau, D., Burovski, E.,  
1140           Peterson, P., Weckesser, W., Bright, J., van der Walt, S. J., Brett, M., Wilson, J., Millman, K.  
1141           J., Mayorov, N., Nelson, A. R. J., Jones, E., Kern, R., Larson, E., ... SciPy 1.0 Contributors.  
1142           (2020). SciPy 1.0: Fundamental algorithms for scientific computing in Python. *Nature*  
1143           *Methods*, 17(3), 261–272. <https://doi.org/10.1038/s41592-019-0686-2>
- 1144   Wang, L. E., Tittgemeyer, M., Imperati, D., Diekhoff, S., Ameli, M., Fink, G. R., & Grefkes, C.  
1145           (2012). Degeneration of corpus callosum and recovery of motor function after stroke: A  
1146           multimodal magnetic resonance imaging study. *Human Brain Mapping*, 33(12), 2941–2956.  
1147           <https://doi.org/10.1002/hbm.21417>
- 1148   Ward, N. S. (2017). Restoring brain function after stroke—Bridging the gap between animals and  
1149           humans. *Nature Reviews Neurology*, 13(4), 244–255.  
1150           <https://doi.org/10.1038/nrneurol.2017.34>
- 1151   Ward, N. S., Brown, M. M., Thompson, A. J., & Frackowiak, R. S. J. (2003a). Neural correlates of  
1152           motor recovery after stroke: A longitudinal fMRI study. *Brain: A Journal of Neurology*,  
1153           126(Pt 11), 2476–2496. <https://doi.org/10.1093/brain/awg245>
- 1154   Ward, N. S., Brown, M. M., Thompson, A. J., & Frackowiak, R. S. J. (2003b). Neural correlates of  
1155           outcome after stroke: A cross-sectional fMRI study. *Brain : A Journal of Neurology*, 126(0 6),  
1156           1430–1448.

- 1157 Ward, N. S., Brown, M. M., Thompson, A. J., & Frackowiak, R. S. J. (2004). The influence of time  
1158 after stroke on brain activations during a motor task. *Annals of Neurology*, *55*(6), 829–834.  
1159 <https://doi.org/10.1002/ana.20099>
- 1160 Ward, N. S., Brown, M. M., Thompson, A. J., & Frackowiak, R. S. J. (2006). Longitudinal changes in  
1161 cerebral response to proprioceptive input in individual patients after stroke: An FMRI study.  
1162 *Neurorehabilitation and Neural Repair*, *20*(3), 398–405.  
1163 <https://doi.org/10.1177/1545968306286322>
- 1164 Ward, N. S., & Cohen, L. G. (2004). Mechanisms Underlying Recovery of Motor Function After  
1165 Stroke. *Archives of Neurology*, *61*(12), 1844–1848.  
1166 <https://doi.org/10.1001/archneur.61.12.1844>
- 1167 Ward, N. S., Newton, J. M., Swayne, O. B. C., Lee, L., Thompson, A. J., Greenwood, R. J., Rothwell,  
1168 J. C., & Frackowiak, R. S. J. (2006). Motor system activation after subcortical stroke depends  
1169 on corticospinal system integrity. *Brain : A Journal of Neurology*, *129*(0 3), 809–819.  
1170 <https://doi.org/10.1093/brain/awl002>
- 1171 Wilke, M., de Haan, B., Juenger, H., & Karnath, H.-O. (2011). Manual, semi-automated, and  
1172 automated delineation of chronic brain lesions: A comparison of methods. *NeuroImage*,  
1173 *56*(4), 2038–2046. <https://doi.org/10.1016/j.neuroimage.2011.04.014>
- 1174 Winters, C., van Wegen, E. E. H., Daffertshofer, A., & Kwakkel, G. (2015). Generalizability of the  
1175 Proportional Recovery Model for the Upper Extremity After an Ischemic Stroke.  
1176 *Neurorehabilitation and Neural Repair*, *29*(7), 614–622.  
1177 <https://doi.org/10.1177/1545968314562115>
- 1178 Woolrich, M., Hunt, L., Groves, A., & Barnes, G. (2011). MEG beamforming using Bayesian PCA  
1179 for adaptive data covariance matrix regularization. *NeuroImage*, *57*(4), 1466–1479.  
1180 <https://doi.org/10.1016/j.neuroimage.2011.04.041>
- 1181 Yamawaki, N., Stanford, I. M., Hall, S. D., & Woodhall, G. L. (2008). Pharmacologically induced  
1182 and stimulus evoked rhythmic neuronal oscillatory activity in the primary motor cortex in  
1183 vitro. *Neuroscience*, *151*(2), 386–395. <https://doi.org/10.1016/j.neuroscience.2007.10.021>

- 1184 Yeo, B. T. T., Krienen, F. M., Sepulcre, J., Sabuncu, M. R., Lashkari, D., Hollinshead, M., Roffman,  
1185 J. L., Smoller, J. W., Zöllei, L., Polimeni, J. R., Fischl, B., Liu, H., & Buckner, R. L. (2011).  
1186 The organization of the human cerebral cortex estimated by intrinsic functional connectivity.  
1187 *Journal of Neurophysiology*, *106*(3), 1125–1165. <https://doi.org/10.1152/jn.00338.2011>
- 1188 Yu, X., Jiaerken, Y., Xu, X., Jackson, A., Huang, P., Yang, L., Yuan, L., Lou, M., Jiang, Q., & Zhang,  
1189 M. (2019). Abnormal corpus callosum induced by diabetes impairs sensorimotor connectivity  
1190 in patients after acute stroke. *European Radiology*, *29*(1), 115–123.  
1191 <https://doi.org/10.1007/s00330-018-5576-y>
- 1192 Zarahn, E., Alon, L., Ryan, S. L., Lazar, R. M., Vry, M.-S., Weiller, C., Marshall, R. S., & Krakauer,  
1193 J. W. (2011). Prediction of Motor Recovery Using Initial Impairment and fMRI 48 h  
1194 Poststroke. *Cerebral Cortex (New York, NY)*, *21*(12), 2712–2721.  
1195 <https://doi.org/10.1093/cercor/bhr047>
- 1196 Zhang, H. Q., Murray, G. M., Turman, A. B., Mackie, P. D., Coleman, G. T., & Rowe, M. J. (1996).  
1197 Parallel processing in cerebral cortex of the marmoset monkey: Effect of reversible SI  
1198 inactivation on tactile responses in SII. *Journal of Neurophysiology*, *76*(6), 3633–3655.  
1199 <https://doi.org/10.1152/jn.1996.76.6.3633>
- 1200 Zhang, H. Q., Zachariah, M. K., Coleman, G. T., & Rowe, M. J. (2001). Hierarchical Equivalence of  
1201 Somatosensory Areas I and II for Tactile Processing in the Cerebral Cortex of the Marmoset  
1202 Monkey. *Journal of Neurophysiology*, *85*(5), 1823–1835.  
1203 <https://doi.org/10.1152/jn.2001.85.5.1823>
- 1204 Zhu, L. L., Lindenberg, R., Alexander, M. P., & Schlaug, G. (2010). Lesion Load of the Corticospinal  
1205 Tract Predicts Motor Impairment in Chronic Stroke. *Stroke*, *41*(5), 910–915.  
1206 <https://doi.org/10.1161/STROKEAHA.109.577023>
- 1207